DOI: 10.1002/marc.((insert number)) ((or ppap., mabi., macp., mame., mren., mats.))

Review

Polymeric Drift Control Adjuvants for Agricultural Spraying

Reece W. Lewis, Richard A. Evans*, Nino Malic, Kei Saito*, Neil R. Cameron*

R.W. Lewis, Dr. K. Saito, Prof. N.R. Cameron
Department of Materials Science and Engineering, Monash University, 22 Alliance Lane, Clayton, 3800, Australia
E-mail: neil.cameron@monash.edu
Dr. K. Saito
School of Chemistry, Monash University, Clayton, 3800, Australia
Dr. R.A. Evans, Dr. N. Malic
CSIRO Manufacturing flagship, Clayton, 3168, Australia

The movement of a pesticide or herbicide to an off-target site during agricultural spraying can cause injury to wildlife, plants and contamination of surface water. This phenomenon is known as spray drift and can be controlled by spraying during favorable environmental conditions, and by using low drift nozzles and drift control adjuvants (DCAs). Polymeric DCAs are the most common type of DCA and function by increasing the droplet size produced during spraying. There are, however, two main drawbacks of polymeric DCAs; they are prone to mechanical degradation during spraying which reduces their performance and they can produce oversized drops which reduces the efficacy of the spray. In this review, existing DCA technology is reviewed including the mechanism through which they function. This then provides a platform for the discussion of novel polymeric architectures which have currently not been applied in DCA formulations.

1. Introduction

The use of pesticides along with genetic improvements in crops largely contributed to a doubling in grain production from 1960 to 2003.[1] While the use of pesticides has a positive influence on crop production, they can also cause adverse effects to surrounding livestock, residents, water and the environment.[2, 3] Spray drift contributes to this undesired effect through the movement of the pesticide spray from the target to any non-target site.[4] Minimising drift has thus received significant interest in an attempt to limit its environmental impact and limit the need for buffer zones between farms.[5] Spray drift is a function of a range of parameters such as wind speed, humidity and droplet size. Of these parameters, droplet size is the most easily controlled and is influenced by the choice of nozzle, operating pressure and composition of spray formulation.[5, 6] In order to reduce spray drift, it is desirable to limit the amount of fine, drift-prone droplets. The size that defines these fine droplets varies depending on the literature source from approximately 50 - 200 μm in volume mean diameter (VMD).[3, 5, 6]

While droplet size is predominantly affected by nozzle selection,[4] polymer adjuvants used in dilute concentration can also strongly affect droplet size and jet breakup.[7] Additionally, these rheology-modifying additives have application in other areas including enhanced oil recovery (EOR),[8] drag reduction in pipelines,[9] cosmetics and inkjet printing.[10, 11] The enhanced extensional viscosity (or elasticity) of polymer solutions is believed to cause the larger drop size.[12] Increases in other rheological properties such as dynamic surface tension,[3, 13] and to a lesser extent static surface tension and zero shear rate viscosity have also been reported to increase spray drop size.[14-16]

There currently exist an extensive range of commercial drift control adjuvants (DCAs), a selection of which is presented in **Table 1**. The majority of commercial DCAs are polymer-based (referred to as spray thickeners), utilising their high elasticity to retard fluid breakup.[17]

Within this classification there are long chain synthetic polymers which include polyacrylamide (PAM), hydrolysed polyacrylamide (HPAM), poly(ethylene oxide) (PEO) and polyvinyl polymers (**Figure 1**).[18, 19] Also included in spray thickeners are polysaccharides such as xanthan gum and guar gum. Many of these polymers have also seen application in EOR and drag reduction.[20] Long chain synthetic polymers are generally able to more significantly reduce fines than polysaccharides, however the latter is more mechanically stable.[21] Mechanical degradation reduces the performance of polymeric DCAs and is a significant weakness in the current technology. PEO has been shown to undergo higher rates of degradation than PAM,[21] which may explain its limited commercial use. Another drawback of spray thickeners is their tendency to shift the entire spray distribution to larger drop sizes. This can reduce the efficacy of the spray due to the formation of oversized drops, which provide poorer coverage.[22, 23]

Inverse emulsions are a class of DCA which tend to give a less significant reduction in fines compared to spray thickeners,[24] however the spray distribution is also narrower which results in fewer oversized drops.[22, 24] Often the emulsions are either vegetable oil- or lecithin-(emulsifying phospholipid) based. Emulsions are reported to increase drop size through a different mechanism to spray thickeners, most notably a shorter spray sheet breakup length is observed.[25, 26] There are other, less common forms of DCAs such as encapsulation based adjuvants,[27] however these will not be discussed here.

This review focuses on the widely used, long chain polymer adjuvants. The performance of various commercial DCAs of this type has been examined in both lab and field studies. For example, two separate studies found that Nalco-Trol (a water-soluble polyvinyl DCA) gave a 63% and 43% increase in VMD compared to water alone when sprayed through flat fan nozzles at 276 kPa.[28, 29] This increase in VMD was shown to considerably reduce drift in a wind tunnel experiment across a range of wind speeds.[28] Many other studies have also found an increase in VMD and reduction in spray drift with the application of polymeric drift

retardants.[19, 23, 30-32] Thus, the design of a DCA with 'long chain polymer' like performance which does not mechanically degrade will be a significant development. Unfortunately it is difficult to use commercial DCA studies to guide the design of future DCAs since details such as polymer molecular weight and specific polymer architecture are often withheld. The following sections will examine the crop spraying process, extensional viscosity and its measurement. Combined, these sections provide an understanding of how polymeric DCAs increase spray droplet size and will provide a platform for the discussion of novel polymeric DCAs including non-linear polymer architectures and associating systems.

2. Agricultural spraying overview

Drift retardant performance and the resultant spray distribution is highly dependent on the conditions employed during spraying. For simplicity, this section will focus on conditions commonly used for large scale boom spraying. These consist of multiple spraying nozzles arranged on a boom which can be attached to a tractor (ground spraying) or aircraft (aerial spraying). For drift minimisation it is desirable to spray at low temperatures (below 30ºC), low relative humidity (less than 40 percent for aqueous solutions) and with a steady wind of 3-15 kmh^{-1} away from sensitive areas.[33] With too high a wind speed the droplets are likely to be carried away from the target site, while without wind a slowly falling dense cloud may form.[33] In order to get appropriate coverage of the agrichemical, the boom height and spray angle needs to be optimised (**Figure 2**). A smaller spray angle or lower boom height results in less drift however it also reduces the coverage of the spray.[34] In general, boom height is between 35 and 100 cm for ground spraying while 3 m is common for aerial sprayers.[3, 35] For some spray solutions a recycle or agitation stream is often diverted from the pump back into the tank in order to achieve a homogeneous or well-mixed spray. This flow tends to be 5 to 10 % of the tank capacity per minute.[36] The average amount of recycle the spray solution will

undergo for agitation varies with spraying speed and other factors, however if, for example, a single tank is to be operated for an hour the spray solution will have undergone an average of 6 recirculations. It should be noted that these recirculations through the pump can degrade significantly a polymeric DCA as is discussed further in section 5. Furthermore, as the tank empties during spraying, the time it takes for the remaining volume to complete a recirculation drops rapidly.[37] This accelerates the degradation process in the latter part of spraying, causing significant variance in droplet spectra from the start to end of application. The recommended spray angle varies with the nozzle type employed, however the range tends to be from 65° to 110°.[34] The spray angle achieved can be reduced by the addition of polymers into the formulation which increase its extensional viscosity. At high concentrations the addition of polymers can lead to the collapse of the spray cone, resulting in a low coverage solid stream exiting the nozzle which is undesirable.[15, 38] The Spray Drift Task Force (set up by the EPA and 38 agrochemical companies to collect data on spray drift) has shown that fluids with an apparent maximum Trouton ratio (indication of extensional resistance, see section 3) of greater than 500 do not properly atomise through some nozzles, reflecting an upper limit in the target extensional viscosity.[39] Finally, the spraying pressure employed also depends on the nozzle, with low pressure devices operating as low as 100 kPa while high pressure nozzles can be in the order of 620 kPa.[40] In general higher pressure results in a finer spray.[41]

There are a range of different nozzle types currently available, with the most common being variants of flat fan, hollow cone, full cone and flood nozzles.[34] Additionally, flat fan and flood nozzles can incorporate a pre-orifice turbulence chamber which causes an internal pressure drop, resulting in a coarser spray with up to 50% less drift than a standard flat fan nozzle. Similarly, the use of venturi or air induction nozzles can further increase spray drop size by incorporating air into the spray, which can result in a 90% drift reduction compared to standard flat fan nozzles. The performance of current DCAs through various nozzles has

revealed some interesting results. Formulations can show a reduction in fines produced through a particular nozzle, while baseline or worse performance is found through another.[6, 27] Additionally, pure water is extensively used as the test carrier fluid in spray testing; however it usually has a larger surface tension than the active formulation which can result in a coarser spray.[15] Thus DCAs should be tested through various nozzle types with appropriate carrier fluid properties to achieve a more complete picture of performance.

The most common measurement of droplet size is VMD, where 50 % of the spray volume is smaller than the reported diameter. This means that numerically there will be more drops of diameter below the VMD since these drops contribute a relatively smaller volume to the overall spray. Also commonly used is Dv0.1 and Dv0.9 where 10 % and 90 % respectively of the spray volume is less than the reported diameter. Thus if, for example, all drops below 150 μm are known to drift and the spray has a Dv0.1 of 150 μm then 10% of the spray volume will be lost to drift.

Agricultural spray atomization is a complex process; the mechanism of droplet formation varies with nozzle type, fluid velocity and fluid physical properties.[42, 43] Firstly, the breakup of jets at low issuing velocities (referred to as the Rayleigh regime) is caused by naturally occurring vibrations in a fluid column which are unstable at certain wavelengths.[44] The amplitude of the unstable disturbances increases along the jet and eventually severs the jet into droplets. The unstable wavelengths and hence stability of these jets depends significantly on the properties of the fluid, with viscoelastic fluids exhibiting a significantly increased breakup length.[7] During jet breakup, viscoelastic fluids display a 'beads-on-a-string' structure; with the droplets connected by thin stretched filaments.[45] These thin filaments are then largely absorbed into the main drops, minimising the formation of satellite droplets and increasing the average droplet size (**Figure 3**).[46, 47] Agricultural spraying is however often carried out at a higher issuing velocity than the Rayleigh regime where the aerodynamic

forces dominate (the atomization regime, **Figure 4**). Here there is complete jet disruption at the nozzle exit, producing droplets with a diameter significantly less than the jet.[48]

A further deviation from simple jet breakup for agricultural spraying is due to the extensive use of flat fan and hollow cone nozzles which produce a liquid sheet rather than a jet.[42, 49] Since both have similar breakup mechanisms,[42] we will focus on flat fan nozzles which have three main breakup mechanisms as listed below.[50-54]

1. Oscillation of waves in the sheet at right angles to the flow which break the sheet into cylindrical ribbons. These ribbons then undergo breakup similar to laminar capillary jets (**Figure 5**).
2. Rim instability where filaments are ripped off the edge of the sheet to form drops (**Figure 6a**).
3. Perforation of the sheet at randomly located points resulting in interconnecting rims known as fluid webs (**Figure 6b**).

When adjuvants conveying elasticity to the fluid are added (such as high molecular weight polymers), breakup by perforation becomes more prominent than with water alone. Additionally the rim is stabilised which minimises drops formed at the edge of the sheet.[55]

All of these mechanisms ultimately result in the formation of thin filaments and it is the breakup of these which has a significant impact on the droplet size spectrum, with thicker filaments reported to produce larger drops.[55] Fluids with enhanced elasticity stabilise and delay the breakup of these filaments in a similar manner to the delayed breakup of jets in the Rayleigh regime.[56, 57] Therefore, although the sheet breakup observed in agricultural spray nozzles is more chaotic than for simple Rayleigh jets, it would appear that the increase in droplet size produced is due to delayed filament breakup in both cases.

In order to better understand the formation of droplets from fluid filaments, a quick overview of filament breakup is now provided. Fluid filaments formed during extension can generally take one of three morphologies as shown in **Figure 7**. The configuration on the right of the

figure with satellite and sub-satellite beads is only possible for viscoelastic (non-Newtonian) fluids, while the other two are possible for both Newtonian (but highly viscous) and non-Newtonian fluids. The satellite droplet is produced at the midpoint of the filament connecting the two main drops, while sub-satellites are formed between the satellite and main drop.[58] Reduction of these non-primary droplets is desirable for drift reduction since they form the smallest droplets in the spray. Understanding and modelling the formation of these satellite and sub-satellite beads is complex and still not fully understood outside of certain ideal cases, however the following trends have been reported for this process. A theoretical modelling study found that fluids with a low Deborah number (De) or low Ohnesorge number (Oh) are more likely to produce multiple beads, including sub-satellites during filament breakup.[59] De is defined in **Equation (1)**, where λ is the characteristic relaxation time of the polymer and t is the characteristic process time. A low De corresponds to a low elasticity, Newtonian-like fluid. Oh represents the ratio of viscous to inertial forces (**Equation 2**), where η_s is the shear viscosity of the fluid, ρ is the density of the fluid, γ is the surface tension of the fluid, L is the characteristic length, Re is the Reynolds number and We is the Weber number. Thus a high inertial component results in low Oh and more sub-satellite bead formation.

$$De = \lambda / t \quad (1)$$

$$Oh = \eta_s / \sqrt{\rho \gamma L} = \sqrt{We} / Re \quad (2)$$

A similar numerical study found that larger Re results in a volumetrically smaller main drop, causing more volume to be found in the satellite and sub-satellite droplets.[60] These studies are thus in agreement since a larger Re results in a smaller Oh. Furthermore the results of these studies would lead to the expectation that lower flow rate (or low spray pressure) and a more elastic fluid will increase the average droplet size of the spray. Since these are experimentally observed phenomena it supports the validity of these studies to agricultural spraying conditions.

Contrasting this, an experimental study found that while polymer adjuvants of very high molecular weight (which have a large De) resulted in a reduction of satellite droplets, a large spike in the number of sub-satellite droplets was observed. These sub-satellite droplets are estimated to be 16 to 60 μm in diameter and are believed to have formed during the breakup of long drawn-out filaments.[61, 62]

Ultimately, in designing a polymeric DCA the reduction in spray efficacy through the formation of oversized drops and the potential increase in sub-satellite droplets need to be taken into account. This should lead to an adjuvant which provides an optimal amount of elasticity to minimize drift and maximise spray efficacy. Polymer solutions are elastic due to their enhanced extensional viscosity, thus an understanding of this complex rheological property is required for novel DCA design. This is the subject of the next section of this review.

3. Extensional viscosity of linear polymer solutions

Polymer solutions are non-Newtonian (often shear thinning), meaning that the shear viscosity is shear-rate dependent.[63] Similarly the extensional viscosity of polymer solutions is extensional-deformation dependent. The intrinsic shear viscosity of a polymer in solution increases with molecular weight according to the Mark-Houwink-Sakurada (MHS) equation (**Equation 3**). M is the molecular weight of the polymer, while α and k depend on the polymer/solvent system.[13] In a good solvent the polymer chains are in a more extended state and as such α is larger in a good solvent than in a theta solvent.[64]

$$[\eta] = kM^{a} \quad (3)$$

Extensional viscosity is a measure of a fluid's resistance to elongational flow, which is the predominant kind of flow found in spray nozzles.[65] As a polymer chain deforms in elongational flow it elongates and aligns in the direction of flow, which leads to an increase in

the frictional interaction between the polymer chains and solvent, hence an increase in extensional viscosity.[66] The Trouton ratio (Tr) is often used to describe this increase and is defined as the ratio of extensional viscosity (η_e) to shear viscosity (η_s) (**Equation 4**). For Newtonian fluids Tr is 3,[67] while, at full extension, polymer solutions can reach a Tr some three orders of magnitude larger.[68]

$$Tr = \frac{\eta_e}{\eta_s} \quad (4)$$

The extensional viscosity increase occurs in elongational flows where the frictional drag force is able to overcome the entropic restoring force of the polymer coil.[69] This strain hardening process occurs at a strain rate corresponding to the coil-stretch transition.[70] The transition is quite sharp since a feedback loop is created with stretching of the chains causing an increased frictional interaction with the surroundings, which in turn further stretches the chains (**Figure 8**).[71] **Equation (5)** describes the critical strain rate for this transition ($\dot{\varepsilon}_{c-s}$), with the Flory exponent (v) varying with solvent and is 0.6 for good solvents and 0.5 for the theta condition.[14]

$$\dot{\varepsilon}_{c-s} \sim M^{-(1-v)} \quad (5)$$

Another more prominent method for estimating the coil-stretch transition involves the Weissenberg number (Wi), which is the ratio of viscous to elastic forces (**Equation 6**). Here $\dot{\varepsilon}$ is the strain rate applied to the polymer solution, with the coil-stretch transition believed to occur for flows at Wi = 0.5.[72-74] The longest relaxation time can be calculated from both Rouse ($\lambda \sim M_w^2$) and Zimm ($\lambda \sim M_w^{1.5}$) models.[75] Both of these models, like Equation (5), point to a decrease in the critical strain rate for coil-stretch transition with an increase in polymer molecular weight. Longer relaxation times also lead to longer filament break-off time, due to the more elastic response.[76] At this point it should be noted that the strain rate experienced by the fluid as it passes through an agricultural spray nozzle has been estimated to be in the order of 10,000 s^{-1}.[20]

$$Wi = \dot{\varepsilon}\lambda \quad (6)$$

Once the chain starts to extend, it is logical to assume that the resistance to elongational flow should be purely a function of strain (extent to which the coil has elongated, **Equation 7**). In this case Hencky (or logarithmic strain) has been defined, where t_r is the residence time, L_0 is the initial length of chain and L_f is the final length of chain. Some literature has supported this conclusion,[77] however more recently this theory has been found to be incomplete. Firstly, it is important to separate the steady-state extensional viscosity (η_e) (resistance at the final, fully extended state) and transient extensional viscosity (η_e^+) (the function which describes how extensional resistance varies in a flow field). McKinley et al.[78] showed that for Wi > 0.5 the transient Trouton ratio (Tr^+) is only a function of strain. However results presented by Gupta et al.[75], suggest that the transient response is only a function of strain for Wi > 6 and that below this it is a function of both strain and strain rate (**Figure 9a**). As is shown in Figure 9a Tr^+ begins to increase from the Newtonian plateau at a Hencky strain of approximately 2 to 3, as has been widely observed.[79] At large strains Tr^+ reaches its maximum value (Tr) and then plateaus, which is a result of the macromolecules no longer extending. This may be due to the chains reaching full extension or perhaps that further extension has been impeded.[80] The strain corresponding to this final plateau varies, although it is often observed at approximately 5 Hencky strain units.[78]

$$\varepsilon = \dot{\varepsilon}t_r = \ln\left(L_f/L_0\right) \quad (7)$$

According to the theoretical Giesekus model Tr (the final steady-state value of Tr^+) is constant for identical polymer solutions, regardless of applied strain rate.[79, 81] This is a logical result since, once the polymer chains are fully elongated, there should be no difference in elongational resistance, no matter what path is taken. However in practice Tr is reduced for flows with very high strain rates; the exact reason for this is still largely unclear with suggestions including the blocking of extension from entanglements,[81] inertial effects and

mechanical degradation.[71] Experimental evidence has shown that high molecular weight polystyrene can undergo significant degradation before reaching the maximum extensional viscosity; further degradation after this point may cause the observed viscosity reduction.[82] A more recent paper using stagnation point flow (see section 4) has suggested that the real cause for this observed lowering in extensional viscosity is the perturbation of flow around the extended polymer chains. This causes the majority of the flow to be diverted around the extended chains at high Tr^+, resulting in an upper limit in the measured pressure drop.[83] This reasoning applies to any technique that measures flow resistance through pressure drop and measures strain rate with a superficial flow velocity. Filament stretching viscometers are one such device which does not measure resistance to flow by pressure drop, rather the force applied to a moving plate. Gupta et al.[75] demonstrated that Tr is reduced when Wi > 10 across a range of molecular weights and concentrations (**Figure 9b**). By re-testing the same fluids and getting almost identical results, the team was able to show that the phenomenon was not due to mechanical degradation. The decrease was attributed to an increase in the number of folded chain structures forming at higher strain rates. These folded chain structures require almost twice the strain to reach full extension (10 strain units), resulting in less extended chains at strains of 5 to 6. Finally, James and Sridhar[80] estimated the strain to full extension (ε_{full}) from **Equation (8)** and were able to show that the measured plateau in Tr^+ occurred at strains below what would be required for full extension. M_0 is the monomer molecular weight and σ is the number of flexible units per link, usually taken as 10. They, along with others, reason that the chains are prevented from achieving full extension by entanglements and knots, and that at higher strain rates disentanglement becomes harder, leading to less extension.[69]

$$\epsilon_{full} \approx 2.5 + \frac{1}{2}\ln\frac{M}{M_O\sigma} \qquad (8)$$

Thus, given the range of plausible explanations for the observed decrease in Tr (steady state) with increasing strain rate, it may eventuate that a combination of these factors is the real

cause. Additionally, given the range of methods used to measure extensional viscosities, the specific cause may be flow field specific.

The value of Tr in dilute polymer solutions increases with polymer molecular weight,[75] which means that increasing polymer molecular weight has a more significant effect on extensional viscosity than shear viscosity after strain hardening. For dilute 1 x 10^5 $gmol^{-1}$ PEO solutions little increase in Tr is observed, with no filament formation observed during jet breakup.[38, 46] Thus there is a minimum molecular weight required to achieve the desired strain hardening behaviour. Indeed, other work has shown evidence of a minimum molecular weight, below which little to no extensional thickening is observed. Testing of various polymer DCAs through a screen viscometer has estimated this value to be close to 5 x 10^5 $gmol^{-1}$,[20] while minimal drag reduction (related to extensional viscosity) is observed in PEO of molecular weight 3 x 10^5 $gmol^{-1}$.[84]

Polymer chain flexibility is also linked to the ability of polymers to undergo strain hardening. Rigid or semi-flexible polymers have higher resistance to extension, therefore the strain hardening behaviour resulting from the coil-stretch transition is sometimes not observed for these polymers.[65] For example, xanthan gums (semi-flexible) have poorer drift retarding performance (un-degraded) than the flexible long chain PAM polymers.[18]

Currently DCAs are generally used in the concentration range of 100 to 1000 ppm, often corresponding to the dilute polymer regime. Dilute solutions are defined as having negligible interactions between neighbouring coils, which occurs below the critical overlap concentration (c*).[81] An important result of this is that for truly dilute solutions, rheological properties such as viscosity should scale linearly with concentration due to the additive nature of each individual chain-solvent interaction.[85] Filament formation is observed below c*, further demonstrating that it is polymer-solvent interactions which result in the observed extensional thickening. c* is inversely proportional to the intrinsic viscosity of the polymer and thus, from Equation (3), c* decreases with increasing polymer molecular weight. c* is

however based on the polymer equilibrium configuration which does not apply for strong extensional flows. This observation led to the definition of 'ultradilute solutions', whose concentration is such that interactions with neighbouring coils is negligible, even during extension.[86] This ultradilute concentration is often found to be approximately 0.1c*, with Brownian simulations predicting that inter-chain interactions are present beyond this point.[87] Experimentally, chain-chain interactions have been observed below c* through a change in the relaxation time of the polymer solution.[13] For example, the relative relaxation times of various polystyrene solutions are plotted in **Figure 10**, demonstrating that for concentrations above 0.1c*, the relaxation time increases relative to the theoretical Zimm relaxation time for a truly dilute solution.[86] Clasen et al.[86] have suggested a scaling of relaxation time with concentration (c) for un-entangled polymer solutions as shown in **Equation (9)**, with v being the solvent quality. Similar power law scaling of relaxation time with concentration for a polysaccharide solution has also been reported, although this study was limited to concentrations greater than c*.[88]

$$\lambda \propto c^{\frac{2-3\nu}{3\nu-1}} \qquad (9)$$

These inter-chain interactions will affect the extensional viscosity or Trouton ratio (both transient and steady state) of a polymer solution in two key ways. Firstly, as the concentration increases it becomes increasingly difficult for the polymer chains to fully extend, which results in a reduced scaling of Tr with concentration beyond the dilute regime. Gupta et al.[75] showed that dilute polystyrene solutions with c/c* between 0.1 and 1 gave an approximately linear increase in Tr with concentration, while in the semi dilute regime just beyond c* a smaller increase in Tr was measured, thought to be due to entanglements. For highly concentrated polystyrene solutions further deviation from the dilute linear scaling was observed, with normalized steady-state extensional viscosity (analogous in definition to Tr) reducing with increasing concentration across a range of strain rates (**Figure 11**).[89] Similar

observations of a decrease in Tr with increasing concentration for concentrated guar gum solutions have also been reported.[90]

The other way in which inter-chain interactions may alter the extensional response of polymer solutions is a lowering of the strain rate required for coil-stretch transition with increasing concentration (due to the increase in relaxation time). This could in theory result in a larger measured transient extensional viscosity, particularly at low strains when the effects of entanglements limiting extension are not as strong. For example, between 5 and 15 times the critical concentration, the Tr^+ of PEO was found to scale with concentration approximately squared.[91] These measurements were limited to strains of approximately 3.5, confirming that these are transient and not steady-state measurements.

Concentration has also been found to influence the filament stretching rheometry filament failure mode (**Figure 12**). For weakly strain hardening concentrated polymer solutions, failure occurs by necking at the mid-plane. In contrast, end plate failure is observed for strongly strain hardening dilute polymer solutions due to the extreme curvature of the filament at the free surface of the plate.[92, 93] This difference in filament failure mode further highlights how higher concentrations can reduce polymer extensibility and hence relative extensional resistance, causing earlier filament break off.

While there is a solid understanding of the effects of polymer molecular weight, concentration and flexibility on the resultant extensional viscosity of a polymer solution, experimental measurement of this property is still required. Accurate and repeatable measurements are difficult to achieve which has resulted in difficulty relating extensional viscosity to the resulting droplet size spectrum, particularly across different studies.[20] For this reason, the following section provides an overview of the methods of measuring extensional viscosity.

4. Measurement of extensional viscosity

In measuring the extensional viscosity of mobile or low viscosity polymer solutions, a vast array of complications has emerged. Imposing a purely elongational flow field with no history of deformation to a mobile fluid is an entirely non-trivial task, with most extensional rheometers not meeting this requirement.[94] Additionally, the extensional viscosity of a fluid is often reported purely as a function of strain rate; however, as discussed in section 3, this is generally not adequate. Unless the residence time of the measuring device is such that equilibrium conditions are reached, extensional viscosity is also a function of time (**Equation 10**). This allows for strain history to be accounted for since the extensional viscosity of a polymer solution is directly related to the extent of uncoiling which has taken place.

$$\eta_e = \eta_e(\dot{\varepsilon}, t) \qquad (10)$$

In general, the following issues are encountered during extensional viscosity measurements.[95]

1. The flow field is not truly extensional (has shear components) or is variable.
2. If strain rate is not constant (in space) an average value may be needed, generating a less meaningful η_e.
3. If steady state is not reached, residence time is not factored in.
4. The flow field is unable to form instantaneously, resulting in effects of pre-history (some chains more strained than others).

In 1989 the test fluid M1 was distributed across multiple research teams in order to compare the measurement techniques of the time, the results of which are compiled in **Figure 13**. This figure highlights that η_e is indeed not just a function of strain rate and that current measurements are simply providing 'an extensional viscosity' rather than the true extensional viscosity.

The M1 project highlighted a clear need for a device which measures the true extensional viscosity, with the main issues of each extensional rheometer summarised in **Table 2**. Shortly after the M1 project, a new filament stretching device was developed by Tritaatmadja and

Sridhar.[77] This device stretches a filament at a controlled and uniform strain rate, with the residence time believed to allow for steady state to be reached. The machine is in general capable of achieving Hencky strains of up to 7, with steady-state extensional viscosity reached at strains of 5 for some test fluids.[80] Larger extensional viscosities for the M1 fluid than reported in the original project were obtained using this technique, a logical result since steady state was apparently reached.

The new technique requires test fluids with a zero shear rate viscosity greater than approximately 1 Pa.s.[96] This has led to most low viscosity fluids (such as DCAs at application concentration) being measured with stagnation point, contraction flow or converging channel methods.[94, 97] Since steady state is often not reached with these measurement types, these values should be referred to as apparent or transient extensional viscosities.[77]

Ultimately, given the complexity of obtaining the extensional viscosity, it may be valid to simply use a technique whose flow field closely matches the application. In the case of flow through a spray nozzle, contraction flows may be used as an approximation. One of the simplest types of contraction flow is found in Screen Factor (SF) testing, where the fluid flows under gravity through a screen pack. Its simplicity has resulted in widespread use of SF measurements as an indication of apparent extensional viscosity and drift retarding ability.[39]

Designing a DCA with an ideal amount of elasticity may allow for significant drift reduction with minimal loss in spray efficacy, however mechanical degradation of high molecular weight polymers can cause variance in the performance throughout the spray cycle. The following section provides an overview of polymer mechanical degradation that can occur during spraying.

5. Mechanical degradation of polymers

The degradation of polymers in both melt and solution through shear or other mechanical agitation has been long known.[98-100] Mechanical degradation is the scission or breakage of polymer chains as a result of built-up mechanical stresses along the polymer chain. The resulting reduction in molecular weight has been observed through a decrease in drag reduction and viscosity of polymer solutions along with GPC and birefringence measurements.[98, 101-103] In the case of agricultural spraying, mechanical degradation can occur as the polymer solution exits the spray nozzle. In fact as is shown in **Figure 14** the desired strain hardening behaviour is often accompanied by mechanical degradation (for contraction flows such as nozzles and porous media) meaning this may be largely unavoidable. As discussed in section 2 a portion of the pumped spray mix is recycled back to the tank during spraying. It is also known that the levels of mechanical stress experienced during a pumping cycle for agricultural sprays are sufficiently large such that dilute polymer solutions can undergo significant degradation. This can then cause an increase in spray drift from beginning to end of spraying when using a polymeric DCA. Since degradation during atomisation is constant throughout the spraying process and fresh polymeric DCAs are known to be effective, degradation caused during pump recirculation is particularly detrimental. For example, with increasing number of cycles through a 3600 RPM centrifugal pump, twelve commercial drift retardants showed a reduction in the droplet size compared to the un-degraded formulation. The number of droplets below 200 μm for a dilute non-ionic PEO solution increased by 355% after 11.4 cycles, with a VMD (after degradation) similar to that produced by pure water.[18]

Increasing linear polymer molecular weight has been shown to increase the extent or probability of chain scission.[104] A molecular weight in the order of 1 x 10^7 $gmol^{-1}$ is often needed for applications in dilute solution drag reduction and drift control, resulting in significant degradation for current additives.[105] It has been observed experimentally that increasing deformation rate increases the rate of chain scission; while a minimum deformation

rate exists, below which no chain scission is observed to occur. For example, a solution of 3 wt% polyisobutene flowing through a capillary only degraded once a critical flow rate was reached.[106] Similarly, dilute poly(vinyl acetate) in toluene was found to undergo minimal scission at 5000 RPM in a homogeniser.[98] This suggests that there is a minimum critical force required for chain scission to occur. Other observed trends include the preferential scission of polymers at the midpoint of the chain and an increase in degradation rate with larger solvent viscosity and higher chain flexibility.[102, 107, 108]

Although this phenomenon is widely reported in the literature as 'shear degradation', it is generally believed that simple laminar shear flow is unable to break polymer chains and that extensional or turbulent flow (which itself contains an extensional element) is required for chain scission to occur.[98, 102, 109] In general, there are two types of elongational flow which are separated by whether or not the residence time (t_r) is greater than the polymer chain relaxation time (λ). Quasi-steady-state elongational flow (QSSF) occurs for $t_r > \lambda$ and as such the polymer chains are able to fully extend. Examples of this include opposed jet and filament stretching devices. Fast transient flow (FTF) has $t_r < \lambda$ resulting in only partially extended polymer chains. FTF commonly arises from flow contraction geometries found in nozzles and valves.[109] A fully extended polymer chain in QSSF can be modelled as a series of hydrodynamic beads linked together by springs. Under the extensional flow, each hydrodynamic bead is pulled away from the centre due to frictional interactions with the surrounding fluid. As shown in **Figure 15** the stresses build up along the chain from each end, with a maximum in the middle of the chain.[110] **Equation (11)** describes how the maximum stress ($\sigma_{c,max}$), observed in the middle of the chain scales with the number of stretched segments (N_l) squared, where ξ is the hydrodynamic drag coefficient.[111]

$$\sigma_{c,max} = \xi b \dot{\varepsilon} {N_l}^2/2 \qquad (11)$$

The frictional loading theory explains a lot of the observed phenomenon for QSSF including preferential mid-chain scission and increase in degradation with solvent viscosity.[112]

Another implication of the frictional loading theory is that there must be a critical strain rate for chain scission to occur, in line with the previously discussed experimental results. The critical strain rate ($\dot{\varepsilon}_c$) is found to scale with molecular weight according to **Equation (12)**.[109] In the case of QSSF the exponent (k) has a value of 2 as can be inferred from Equation (11). However in FTF, where the chains are not fully extended, the exponent decreases to 1. Another significant deviation of FTF experimental results from the frictional loading model is the significantly lower frictional breaking force measured compared to the known breaking strength of C-C bonds.[112, 113] These results imply that the mechanism for chain scission is dependent on the flow conditions employed.[114]

$$\dot{\varepsilon}_c \propto M^{-k} \qquad (12)$$

The lower measured breaking strength could also be influenced by the formation of knots, which has been shown to cause a structural weakness. Here, bond breakage usually occurs at the entrance of the knot and can reduce the energy stored in the chain at breakage from 67.8 kJmol^{-1} for a linear chain to 53.1 kJmol^{-1} for a knotted chain.[115] Knot theory states that the chance of finding a knot in a polymer modelled as a self-avoiding walk approaches one as the number of monomers increases.[116] Knots are highly unlikely to form in a chain with a degree of polymerisation (DP) of 150 [117], increasing the chain size increases this chance and at a DP of order 10^5 the chance of finding a knot is considered likely.[116] For PAM this corresponds to a molecular weight between 1 x 10^4 gmol^{-1} and 7 x 10^6 gmol^{-1}. Since most DCAs have a molecular weight in the millions, it is possible that knots could contribute to this lower bond strength.

Due to the promising application of these high molecular weight rheology modifying polymers, extensive research has been conducted into improving the mechanical stability of polymers in solution. Polymers that form networks through associations and entanglements with neighbouring chains display increased mechanical stability. This is believed to be due to the distribution of the stresses over multiple chains and the sacrificial breakage of physical

bonds in the network over chemical bonds along the main chain.[18, 105, 118] Following on from this, a prominent design philosophy for mechanically stable polymers involves the use of lower molecular weight polymers (which are less susceptible to degradation) which can then assemble into higher molecular weight polymer chains through non-covalent interactions. Successful application of this could result in a polymeric DCA with consistent drift control performance from beginning to end of spraying due to only the non-covalent bonds being broken during pump recirculation (which can then be reformed in the tank). These networks may be formed through entanglements, ionic attractions and hydrophobic/ hydrophilic interactions as will be discussed in detail in the following section. Branched polymers have also shown enhanced mechanical stability through the preferential scission of branching structures over the main chain which results in a less significant reduction of molecular weight. Application of these and other non-linear polymer morphologies is examined in the final section.

6. Polyelectrolytes

Polyelectrolytes are the most widely used associating polymer in current DCAs. Polyelectrolyte polymers are those with anionic or cationic groups along the chain, which cause intra- and intermolecular interactions.[119] Polymer chains with like charges expand from electrostatic repulsions, leading to an increase in inter-chain entanglements.[120, 121] The increased entanglements give polyelectrolytes their network/ associative characteristic, although the formation of charged complexes with multivalent ions in solution may also be a factor.[122] The fraction of charged monomers along the polymer chain is denoted as α. Some of these charged monomers will be shielded by charge condensation due to their counterions. Effective charges along the polymer are those charges that have not been shielded. The

fraction of effective charges is denoted as f, and in the case of very dilute solutions, f approaches α since there is minimal charge shielding.[123]

Polyelectrolytes adopt extended long chain conformations through the formation of 'electrostatic blobs' that repel each other (**Figure 16**). This property results in a lower critical concentration of polyelectrolytes compared to neutral polymers, with the reduction scaling with increasing f. For example, one such study found the critical concentration of a highly charged polyelectrolyte to be 1/30 of its analogous neutral polymer.[123] Approaching the critical concentration, both charged and neutral polymers had similar solution viscosity despite the charged polymer being of significantly lower concentration.

Various promising experimental results for the use of polyelectrolytes as rheology modifiers have emerged. Zhu et al.[18] tested various commercial drift retardants and found that the anionic polymer additives as a group experienced less mechanical degradation than their non-ionic counterparts. The best performing polymer additive in terms of measured droplet sizes below 200 μm both before and after shearing was a 20 mol% anionic PAM. Another study compared cationic, anionic and non-ionic PAM and found that steady-state extensional viscosity was the main variable in determining amount of spray lost to drift, with little variance between polymer types.[14] Given that the polymers used in the study by Zhu et al. were of variable molecular weight (and hence extensional viscosity) it is likely that there is minimal difference across non-degraded ionic and non-ionic polymers. The improved shear stability, however, has been further shown across studies for use in EOR and drag reduction.[124, 125] The solvents used in the above-mentioned studies were distilled water, water, 1M NaCl solution and kerosene respectively. These results reflect the diverse applicability of polyelectrolytes although increasing salt concentration does reduce the effect, as will be discussed. The mechanical stability of polyelectrolytes has been attributed to the formation of intermolecular networks in all the above studies. Additionally, the charged

groups on polyelectrolytes reduce the flexibility of the polymer chain, which may also contribute to the improved stability.[108]

At polymer concentrations above the critical overlap concentration, the electrostatic interactions are increasingly shielded through an increase in concentration of counterions. A similar effect is achieved through the addition of salts into the polymer solution. This is reflected in a study which compared the mechanical degradation of polyacrylamides. In distilled water there was a significant improvement in the shear stability of the polyelectrolyte HPAM compared to the non-ionic PAM. In fact there was no evident degradation for a 1.5g/L HPAM solution at a shear rate of 80,000 s^{-1}. With the introduction of NaCl to the solution HPAM underwent degradation. The amount of NaCl added was increased from 0.2 to 1 wt%, with rates of chain scission increasing accordingly.[111] Thus the addition of ions to the solution results in charge shielding of the polyelectrolyte and a reduction in the level of entanglements and associations which weakens the network. This presents an issue since spray tank mixes often contain additional sources of ions (for example ionic surfactants).

7. Future Directions

Hydrophobic and hydrophilic interactions have not been applied in current DCA formulations, however these non-covalent interactions could also be used in the formation of a dynamic and reformable network. This network can then mimic the desired strain hardening behaviour of a higher molecular weight polymer, while undergoing less permanent deformation during the pumping cycle. Importantly, these interactions are largely not affected by the presence of ions in solution.[126] In fact the 'salting out' phenomenon actually makes the aqueous system more hostile to hydrophobes with addition of salt, leading to stronger hydrophobic interactions.[127] These hydrophobically associating polymers tend to be either in the form of a telechelic (hydrophobic groups on either end of a hydrophilic polymer) or a

multi-sticker polymer (hydrophobic groups randomly grafted along a hydrophilic chain) as shown in **Figure 17**. Both of these form bridged multiplets which can consist of intra- and intermolecular associations.[128, 129] Reportedly, the multi-sticker polymers have enhanced viscosity improvement over telechelics due to the increase in the number of bridges formed across the multiplets.[130] Similarly, the combination of the two (multisticker with hydrophobic groups at the end) is said to be optimal for polymers in EOR and so also could be beneficial as DCAs.[122] The extent of intra- and intermolecular associations as well as the extent of hydrophobic modification has an effect on the solution rheology.[131] This is on top of standard factors such as concentration, chain flexibility and molecular weight. In fact concentration has a particularly pronounced effect on the rheology of hydrophobically associating polymers since it also determines the relative amounts of intra- and intermolecular associations. Below the critical association concentration (c_a*) intramolecular associations dominate since the chains do not interact with each other.[132] This can lead to similar or even smaller viscosity than an unmodified polymer due to bunching up of the chains.[133] Tan et al.[131] found that 0.3 and 0.5 wt% solutions of HASE (hydrophobically alkali-soluble associative) polymers had near constant Tr across a range of extensional rates, while once the concentration was increased to 0.8 wt%, Tr increased strongly with extensional rate. The results of this are in line with an earlier paper looking at a similar hydrophobically associating polymer, which also found minimal increase in Tr with increasing strain rate at concentrations at or below 0.5 wt%.[134] This reflects the highly concentration sensitive nature of the rheology for hydrophobically associating polymers.

Upon increasing the concentration beyond c_a* the solution enters the semi-dilute regime. Here the modified associating polymer displays enhanced shear and extensional viscosity over an unmodified polymer. This regime is defined between c_a* and the entanglement concentration (c_e), which is typically 5 to 10 times c_a* [133]. This increase in viscosities is due to the increasingly favoured formation of intermolecular bonds in the semi-dilute regime.

Additionally these solutions tend to initially undergo shear and strain thickening due to the further formation of intermolecular associations over intramolecular interactions. The onset of strain thickening has been reported at a modified Weissenberg number of 0.1, lower than that for an unmodified polymer (0.5).[135] The modified Weissenberg number is defined in terms of its effective relaxation time (λ_{eff}) (**Equation 13**) which is altered by the presence of hydrophobic groups. This hydrophobic interaction is reflected through the relaxation time scaling with concentration (along with molecular weight), which is not the case for non-associating linear polymers below c* (which only scale with molecular weight).[136] At higher rates of shear and strain, a thinning behaviour is observed due to degradation of the network forming hydrophobic interactions between chains. The strain rate of thinning often occurs between a modified Weissenberg number of 1 and 3.[135]

$$\lambda_{eff} \sim (c\sqrt{M})^{2/3} \qquad (13)$$

While concentration has a significant influence on the nature of the hydrophobic interactions, the hydrophobicity of the associating group influences the strength of the network. Increasing hydrophobic group length increases the strength of the bridges formed in the network and hence increases the extensional and shear viscosities while decreasing the critical concentration.[134] There is however a limit imposed by solubility, with too many hydrophobic groups on the chain leading to phase separation and insolubility.[131]

Since most rheology modifiers are used at very low concentrations, a novel set of multi-sticker associating chains with a set of donor-acceptor functional groups was developed. The hypothesis was that if only intermolecular associations are possible by design, problematic intramolecular complexes formed at concentrations below the critical concentration could be eliminated. This solution comprised of a mixture of carboxylic acid-functionalised polymers and those with a complementary tertiary amine group (**Figure 18**). These polymer mixtures were tested in terms of their droplet breakup characteristics, showing no noticeable filament formation and less evidence of extensional thickening than an un-paired (self-associating)

polymer. This was attributed to the formation of large dense clusters with increased segment density, limiting the ability of the chains to expand.[105]

While linear polymers have been applied in the majority of current drift retardants, various other polymer architectures such as comb, star and dendritic polymers are available and some of these are currently employed in EOR and so could also find application as DCAs. Typically, these branched polymers have a lower radius of gyration and viscosity when compared to a linear analogue of equal total molecular weight.[137, 138] This is due to the increased density of polymer chains in branched morphologies. It is often convenient to compare these structures by a branching factor (g'), defined as the ratio of intrinsic viscosity of the branched polymer ($[\eta]_B$) divided by that of a linear polymer ($[\eta]_L$) with equal molecular weight (**Equation 14**).[139]

$$g' = [\eta]_B/[\eta]_L \quad (13)$$

The branching factor tends to increase with the molecular weight of arms and decrease with the number of arms.[139, 140] Similar effects are seen in extensional properties by polymer solution modelling where increasing the number of arms (at constant arm length) results in a later coil-stretch transition and a lower extensional viscosity even at high strain rates.[141] Similarly, modelling has shown that increasing the arm length (with constant number of arms) leads to a larger extensional viscosity.[142] There are currently limited experimental studies on the extensional viscosity of branched polymers in solution. It is possible however to understand the effects of such structures on molecular interaction by examining the changes in shear viscosity. By comparing the shear viscosity of star, comb and linear polymers with similar span molecular weight (weight of molecules comprising the longest linear section in any architecture) it was found that comb polymers displayed the highest viscosity, followed by star polymers. Although less significant, comb polymers were even found to have a larger shear viscosity than linear polymers when compared by total molecular weight at

concentrations above 5 wt% (and approximately equal below 5 wt%). This viscosity enhancement was attributed to additional entanglements caused by the architecture of comb and star polymers.[143] Increasing the span molecular weight increased the difference between branched and linear polymers, in line with theory which states that the viscosity of branched structures increases exponentially with molecular weight, while linear polymers follow a power law (Equation 3).[144]

These results contrast with earlier work which suggested that the viscosity of branched polymers is always less than that of a linear polymer of equal total molecular weight. An explanation may be found in the large arm molecular weight of the polymers tested in the above study, which ranged from 3 x 10^3 to 5 x 10^4 $gmol^{-1}$. Each comb consisted of 12 branching sites on an approximately 3 x 10^3 $gmol^{-1}$ macroinitiator.[143] At up to 5 x 10^4 $gmol^{-1}$ these arms are significantly larger than those used in the earlier study, which were at most 1 x 10^4 $gmol^{-1}$.[137] Their results also showed that increasing the number of branches at constant total molecular weight decreases the branching factor which can be attributed to a lower arm molecular weight and a more compact, dense structure. Dense structures are known to be detrimental in terms of viscosity, for example the branching factor of comb-on-comb polymers is very small, which is attributed to their densely packed nature.[145] Additionally, core cross-linked star polymers have been shown to have a low branching factor, which is likely caused by the dense core containing 10-30% of the polymer mass.[139] Dendrimers are another commonly explored polymer morphology with a dense structure due to the high degree of branching. The rheological properties of dendrimers reflect this with a critical molecular weight (or number of generations) beyond which the intrinsic viscosity of the polymer actually decreases. This signifies a transition from an open structure to a more compact globular polymer.[146, 147] A theoretical investigation of combs with larger side chain length than backbone segment length demonstrated that the polymers exhibit a more stretched conformation due to steric interference.[148] The conformation of branched polymers is also

highly dependent on the solvent (like all polymers), with poor solvents resulting in a collapsed, spherical-like structure for comb polymers.[148]

Star-like dendrimers have a lower degree of branching than standard dendrimers and as such a more open structure. For up to three generations, a branching factor of greater than one was found for star-like dendrimers of polystyrene with an arm molecular weight of 4,300 $gmol^{-1}$ (between each generation). Star-like dendrimers with smaller arm length displayed smaller branching factors. These results reinforce the need for long branching and open structures for viscosity enhancement.[149]

Enhanced mechanical stability for branched polymers has also been reported. Experimental studies have compared star and linear PAM of similar 'drag reduction potential' and HPAM of same initial molecular weight. [111, 150] In both cases the star morphology gave superior resistance to mechanical degradation. These results are in part attributed to the known phenomenon of preferential branch scission over the main chain links, which results in a relatively lower reduction in molecular weight. Modelling has shown that it is more likely to be arm fragmentation rather than removal of the entire branch, further adding to this effect.[104] The arm fragmentation model is backed up by experimental results comparing the shear stability of fused core star polymers and linear core star polymers. In theory, linear core star polymers experience a larger stress at the core, however there was minimal degradation difference found between the two.[110] This pointed to arm fragmentation being the main mechanism of degradation since the bond strengths along the arm are equal for both stars.

Limited extensional viscosity measurements have been performed on branched polymers in dilute solutions. The application of a high molecular weight comb polymer in EOR was investigated with comparison to a linear sample. The comb polymer consisted of a polyelectrolyte backbone with short side chain hydrophobic groups which caused steric and electrostatic repulsion, resulting in a more extended conformation. The comb polymer had

consistently higher extensional viscosity and was shown to recover more oil than a linear comparator.[151]

Although not currently applied to drift control, it appears that combining the effects of polyelectrolytes and hydrophobic associations in a comb-like structure is a promising method for producing mechanically stable DCAs. These structures can have a pH sensitive conformation due to the polyelectrolyte backbone. **Figure 19** highlights how altering the pH and thus ionising the backbone causes an increase in intermolecular associations.[152] This chain expansion helps overcome a significant issue for conventional hydrophobic polymers, which otherwise require a relatively high concentration for association and network formation.[153] For example, amphiphilic branches with a hydrophilic PEO segment and hydrophobic aliphatic carbon segment have been synthesised.[152] Similarly, a non-ionic amphiphilic branched polymer was developed for use in EOR since the electrostatic repulsions are usually shielded by the salt present in this application. The branches consisted of hydrophilic PEO and a hydrophobic t-octyl group. The hydrophilic segment increases solubility and allows freedom of movement for the associating hydrophobic group. The hydrophobic segment gives intermolecular interactions and is the source of a repulsive interaction causing the chains to unfold (in absence of the polyelectrolyte).[154]

8. Conclusions

Spray drift is a function of an extensive set of parameters, of which droplet size is the most significant and easily controllable. By reducing the amount of fine or small droplets in the spray, a significant reduction in drift can be achieved. Viscoelastic fluids stabilise filaments formed during spray sheet breakup and are known to supress the formation of fine droplets. Dilute, high molecular weight polymers display this behaviour and many commercially available DCAs are of this type. In developing the next generation of DCAs, focus on

mechanically stable polymers with an optimal extensional viscosity which limits satellite droplet formation while retaining significant chemical spray coverage will be vital. High molecular weight polymer chains are particularly susceptible to mechanical degradation, which reduces the molecular weight of the polymer and hence its drift retarding potential. Mechanical degradation can be limited by the formation of polymer networks in the solution which allow for distribution of the stresses. Polyelectrolytes have shown improved mechanical stability through the formation of more rigid extended polymer chain networks; however, these are less effective in high salt concentration solutions which act to shield the ionic interactions. Intermolecular hydrophobic associations are not limited by salt content, however at low concentrations the hydrophobic groups on polymer chains tend to preferentially self-associate, leading to a reduction in viscosity. Branched structures such as combs and stars also offer improved mechanical stability through preferential arm fragmentation which leads to a smaller reduction in molecular weight. Combining polyelectrolytes with hydrophobically associating comb polymers could lead to synergistic effects due to the chain expansion caused by charge repulsion along the backbone and network formation from the hydrophobic groups on the comb branches.

Nomenclature/Abbreviations

c	Polymer concentration	t	Characteristic process time
c*	Critical overlap concentration	t_r	Residence time
c_a*	Critical association concentration	Tr	Trouton ratio ($=\eta_e/\eta_s$)
DCA	Drift Control Adjuvant	Tr^+	Transient Trouton ratio ($=\eta_e^+/\eta_s$)
De	Deborah number ($=\lambda/t$)	v	Velocity (of flow)
EOR	Enhanced oil recovery	VMD	Volume mean diameter
f	Fraction of effective charges	We	Weber number ($=v^2\rho L/\gamma$)
FTF	Fast transient flow ($t < \lambda$)	Wi	Weissenberg number ($=\dot{\varepsilon}\lambda$)
g’	Branching factor	α	Fraction of charged monomers
HPAM	Hydrolysed polyacrylamide	γ	Surface tension

L	Characteristic length	λ	Characteristic relaxation time
L_f	Final polymer length	ε	Strain ($=\ln(L_f/L_0)$)
L_0	Initial polymer length	$\dot{\varepsilon}$	Strain rate
M	Polymer molecular weight	$\dot{\varepsilon}_c$	Critical strain rate
M_0	Monomer molecular weight	ε_{full}	Strain to full extension
N_l	Number of stretched segments	ξ	Hydrodynamic drag coefficient
Oh	Ohnesorge number ($=\eta_s/(\gamma\rho L)^{1/2}$)	$[\eta]$	Intrinsic shear viscosity
PAM	Polyacrylamide	η_e	Extensional viscosity
PEO	Poly(ethylene oxide)	η_e^+	Transient extensional viscosity
QSSF	Quasi-steady-state elongational	η_s	Shear viscosity
	flow ($t > \lambda$)	λ_{eff}	Effective relaxation time
Re	Reynolds number ($=v\rho L/\eta_s$)	λ_Z	Longest Zimm relaxation time
SF	Screen factor	ρ	Density
		$\sigma_{c,max}$	Maximum stress on polymer

Acknowledgements: The Ph.D position of RWL was supported by the Chemicals and Plastics Manufacturing Innovation Network and Training Program at Monash University.

Received: Month XX, XXXX; Revised: Month XX, XXXX; Published online:

((For PPP, use "Accepted: Month XX, XXXX" instead of "Published online")); DOI: 10.1002/marc.((insert number)) ((or ppap., mabi., macp., mame., mren., mats.))

Keywords: viscoelastic properties, degradation, solution properties, polyelectrolytes, branched

References

[1] E. C. Oerke, *Journal of Agricultural Science* **2006**, *144*, 31.
[2] R. Peshin, A. K. Dhawan, D. Pimentel, *Integrated pest management*, Springer, Dordrecht, **2009**.
[3] A. S. Felsot, J. B. Unsworth, J. B. H. J. Linders, G. Roberts, D. Rautman, C. Harris, E. Carazo, *Journal of Environmental Science and Health, Part B* **2010**, *46*, 1.
[4] M. Al Heidary, J. P. Douzals, C. Sinfort, A. Vallet, *Crop Protection* **2014**, *63*, 120.
[5] E. Hilz, A. W. P. Vermeer, *Crop Protection* **2013**, *44*, 75.
[6] P. Spanoghe, M. De Schampheleire, P. Van der Meeren, W. Steurbaut, *Pest Management Science* **2007**, *63*, 4.
[7] R. P. Mun, J. A. Byars, D. V. Boger, *Journal of Non-Newtonian Fluid Mechanics* **1998**, *74*, 285.
[8] A. Zaitoun, P. Makakou, N. Blin, R. S. Al-Maamari, A.-A. R. Al-Hashmi, M. Abdel Goad, H. H. Al-Sharji, *SPE Journal* **2012**.
[9] M. Stelter, T. Wunderlich, S. K. Rath, G. Brenn, A. L. Yarin, R. P. Singh, F. Durst, *Journal of Applied Polymer Science* **1999**, *74*, 2773.
[10] A. Laschewsky, C. Herfurth, A. Miasnikova, F. Stahlhut, J. Weiss, C. Wieland, E. Wischerhoff, M. Gradzielski, P. M. de Molina, *Acs Sym Ser* **2013**, *1148*, 125.
[11] S. D. Hoath, I. M. Hutchings, G. D. Martin, T. R. Tuladhar, M. R. Mackley, D. Vadillo, *Journal of Imaging Science and Technology* **2009**, *53*, 041208.
[12] A. N. Rozhkov, *Fluid Dynamics* **2005**, *40*, 835.
[13] V. Tirtaatmadja, G. H. McKinley, J. J. Cooper-White, *Physics of Fluids* **2006**, *18*.
[14] P. A. Williams, R. J. English, R. L. Blanchard, S. A. Rose, L. Lyons, M. Whitehead, *Pest Management Science* **2008**, *64*, 497.
[15] A. J. Hewitt, A. J. Stern, W. E. Bagley, R. Dexter, in *Pesticide Formulations and Application Systems: Global Pest Control Formulations for the Next Millennium*, Vol. 19 (Eds: R.S. Tann, J.D. Nalewaja, and A.K. Viets), ASTM International, Mayfield, USA, **1999**, p. 135.
[16] N. Ashgriz, A. L. Yarin, in *Handbook of Atomization and Sprays: Theory and Applications*, Vol. 1 (Ed: N. Ashgriz), Springer, New York, USA, **2011**, p. 3.
[17] P. M. McMullan, *Weed Technology* **2000**, *14*, 792.

[18] H. Zhu, R. W. Dexter, R. D. Fox, D. L. Reichard, R. D. Brazee, H. E. Ozkan, *Journal of Agricultural Engineering Research* **1997**, *67*, 35.
[19] H. Guler, H. Zhu, E. Ozkan, R. Derksen, C. Krause, *Pesticide Formulations & Delivery Systems, 26 Vol: Reassessing Pesticide Technologies* **2008**, *1478*, 72.
[20] R. W. Dexter, *Atomization and Sprays* **1996**, *6*, 167.
[21] A. Summervaille, G. Betts, B. Gordon, V. Green, M. Burgis, R. Henderson, *Adjuvants – Oils, surfactants and other additives for farm chemicals – revised 2012 edition*, Grains Research and Develpment Corporation, Kingston, Australia, **2012**.
[22] K. Penfield, A. Halecky, in *Pesticide Formulation and Delivery Systems*, Vol. 33, STP 1569 (Ed: C. Sesa), ASTM International, West Conshohocken, **2014**, p. 1.
[23] J. E. Hanks, *Weed Technology* **1995**, *9*, 380.
[24] Y. Lan, W. C. Hoffmann, B. K. Fritz, D. E. Martin, J. D. Lopez, *Applied Engineering in Agriculture* **2008**, *24*, 5.
[25] C. F. Creech, "Herbicide application technology impacts on herbicide spray characteristics and performance", in *ProQuest Dissertations and Theses*, University of Nebraska, **2015**, p. Ph.D./220.
[26] P. C. H. Miller, A. J. Hewitt, W. E. Bagley, in *Pesticide Formulations and Application Systems*, Vol. 21, STP 1414 (Eds: J.C. Mueninghoff, A.K. Viets, and R.A. Downer), ASTM International, West Conshohocken, **2001**, p. 175.
[27] A. K. Johnson, F. W. Roeth, A. R. Martin, R. N. Klein, *Weed Technology* **2006**, *20*, 893.
[28] H. E. Ozkan, D. L. Reichard, H. P. Zhu, K. D. Ackerman, in *Pesticide Formulations and Application Systems*, Vol. 13, STP 1183 (Eds: P.D. Berger, B.N. Devisetty, and F.R. Hall), ASTM International, Philadelphia, **1993**, p. 173.
[29] A. C. Chapple, R. A. Downer, F. R. Hall, *Crop Protection* **1993**, *12*, 579.
[30] A. Sundaram, K. M. S. Sundaram, A. G. Robinson, W. J. G. Beveridge, J. W. Leung, *Transactions of the Asae* **1992**, *35*, 387.
[31] L. F. Bouse, J. B. Carlton, P. C. Jank, *Transactions of the ASAE* **1988**, *31*, 1633.
[32] S. A. H. Rose, L. Lyons, M. Whitehead, *Pesticide Formulations & Delivery Systems, 26 Vol: Reassessing Pesticide Technologies* **2008**, *1478*, 20.
[33] *Spray Drift Managment Principals, Strategies and Supporting Information*, CSIRO Publishing, **2002**.
[34] M. P. Johnson, L. D. Swetnam, *Sprayer Nozzles: Selection and Calibration*, University of Kentucky, Lexington, **1996**.
[35] H. J. Holterman, J. C. van de Zande, H. A. J. Porskamp, J. F. M. Huijsmans, *Computers and Electronics in Agriculture* **1997**, *19*, 1.
[36] R. D. Grisso, D. L. Varner, R. N. Klein, "G91-1020 Plumbing Systems of Agricultural Sprayers", in *Histrical Materials from University of Nebraska- Lincoln Extension*, University of Nebraska-Lincoln, **1991**, p. Paper 701/.
[37] A. C. Chapple, R. A. Downer, F. R. Hall, in *Pestacide Formulations and Application Systems*, Vol. 11, STP 1112 (Eds: L.E. Bode and D.G. Chasin), ASTM International, Philadelphia, **1992**, p. 193.
[38] R. P. Mun, B. W. Young, D. V. Boger, *Journal of Non-Newtonian Fluid Mechanics* **1999**, *83*, 163.
[39] R. W. Dexter, *Pesticide Formulations & Delivery Systems, 26 Vol: Reassessing Pesticide Technologies* **2008**, *1478*, 3.
[40] T. Wolf, *Prairie Soils and Crops* **2009**, *2*, 24.
[41] E. J. Jones, J. E. Hanks, G. D. Wills, R. E. Mack, *Weed Technology* **2007**, *21*, 171.
[42] P. C. H. Miller, M. C. Butler Ellis, *Crop Protection* **2000**, *19*, 609.
[43] A. H. Lefebvre, *Atomization and sprays*, Taylor & Francis, New York, **1989**.
[44] L. Rayleigh, *Proceedings of the Royal Society of London* **1879**, *29*, 71.

[45] L. Han, D. Doraiswamy, R. K. Gupta, *Journal of Thermal Analysis and Calorimetry* **2011**, *106*, 305.
[46] Y. Christanti, L. M. Walker, *Journal of Rheology* **2002**, *46*, 733.
[47] C. Wagner, Y. Amarouchene, D. Bonn, J. Eggers, *Physical Review Letters* **2005**, *95*, 164504.
[48] C. Dumouchel, *Experiments in Fluids* **2008**, *45*, 371.
[49] M. C. B. Ellis, C. R. Tuck, *Crop Protection* **1999**, *18*, 101.
[50] V. Bergeron, *Comptes Rendus Physique* **2003**, *4*, 211.
[51] N. Dombrowski, R. P. Fraser, *Philosophical Transactions of the Royal Society of London, Series A: Mathematical and Physical Sciences* **1954**, *247*, 101.
[52] M. C. B. Ellis, C. R. Tuck, P. C. H. Miller, *Crop Protection* **1997**, *16*, 41.
[53] R. G. Dorman, *British Journal of Applied Physics* **1952**, *3*, 189.
[54] R. E. Ford, C. G. L. Furmidge, *British Journal of Applied Physics* **1967**, *18*, 335.
[55] J. C. Thompson, J. P. Rothstein, *Journal of Non-Newtonian Fluid Mechanics* **2007**, *147*, 11.
[56] G. Y. Park, G. M. Harrison, *Atomization and Sprays* **2008**, *18*, 243.
[57] M. Negri, H. K. Ciezki, S. Schlechtriem, *EUCASS Proceedings Series – Advances in AeroSpace Sciences* **2013**, *4*, 271.
[58] M. Tjahjadi, H. A. Stone, J. M. Ottino, *Journal of Fluid Mechanics* **1992**, *243*, 297.
[59] P. P. Bhat, S. Appathurai, M. T. Harris, M. Pasquali, G. H. McKinley, O. A. Basaran, *Nature Physics* **2010**, *6*, 625.
[60] A. M. Lakdawala, R. Thaokar, A. Sharma, *Chemical Engineering Science* **2015**, *130*, 239.
[61] Y. Christanti, L. M. Walker, *Journal of Non-Newtonian Fluid Mechanics* **2001**, *100*, 9.
[62] X. G. Zhang, O. A. Basaran, *Physics of Fluids* **1995**, *7*, 1184.
[63] J. F. Ryder, J. M. Yeomans, *Journal of Chemical Physics* **2006**, *125*.
[64] M. R. Kasaai, *Carbohydrate Polymers* **2007**, *68*, 477.
[65] G. M. Harrison, R. Mun, G. Cooper, D. V. Boger, *Journal of Non-Newtonian Fluid Mechanics* **1999**, *85*, 93.
[66] J. A. Odell, S. P. Carrington, in *Flexible Polymer Chains in Elongational Flow* (Eds: T. Nguyen and H.-H. Kausch), Springer Berlin Heidelberg, **1999**, p. 137.
[67] J. Ferguson, N. E. Hudson, B. C. H. Warren, *Journal of Non-Newtonian Fluid Mechanics* **1992**, *44*, 37.
[68] T. Sridhar, V. Tirtaatmadja, D. A. Nguyen, R. K. Gupta, *Journal of Non-Newtonian Fluid Mechanics* **1991**, *40*, 271.
[69] N. V. Orr, T. Sridhar, *Journal of Non-Newtonian Fluid Mechanics* **1996**, *67*, 77.
[70] S. L. Anna, G. H. McKinley, *Rheologica Acta* **2008**, *47*, 841.
[71] J. A. Odell, S. P. Carrington, *Journal of Non-Newtonian Fluid Mechanics* **2006**, *137*, 110.
[72] T. Lim, J. T. Uhl, R. K. Prud'homme, *SPE Reservoir Engineering* **1986**, *1*, 272.
[73] G. H. Mckinley, *The British Society of Rheology* **2005**, 1.
[74] M. Chellamuthu, D. Arora, H. H. Winter, J. P. Rothstein, *Journal of Rheology* **2011**, *55*, 901.
[75] R. K. Gupta, D. A. Nguyen, T. Sridhar, *Physics of Fluids* **2000**, *12*, 1296.
[76] S. D. Hoath, D. C. Vadillo, O. G. Harlen, C. McIlroy, N. F. Morrison, W. K. Hsiao, T. R. Tuladhar, S. Jung, G. D. Martin, I. M. Hutchings, *Journal of Non-Newtonian Fluid Mechanics* **2014**, *205*, 1.
[77] V. Tirtaatmadja, T. Sridhar, *Journal of Rheology* **1993**, *37*, 1081.
[78] G. McKinley, S. Anna, A. Tripathi, M. Yao, presented at *15th Annual Meeting of the International Polymer Processing Society*, Netherlands, (May, **1999**)

[79] M. W. Yao, S. H. Spiegelberg, G. H. McKinley, *Journal of Non-Newtonian Fluid Mechanics* **2000**, *89*, 1.
[80] D. F. James, T. Sridhar, *Journal of Rheology* **1995**, *39*, 713.
[81] R. G. Larson, *Complex Systems* **2008**, *982*, 419.
[82] R. Haas, W. M. Kulicke, in *The Influence of Polymer Additives on Velocity and Temperature Fields* (Ed: B. Gampert), Springer Berlin Heidelberg, **1985**, p. 119.
[83] S. J. Haward, J. A. Odell, Z. Li, X. F. Yuan, *Rheologica Acta* **2010**, *49*, 781.
[84] A. S. Pereira, E. J. Soares, *Journal of Non-Newtonian Fluid Mechanics* **2012**, *179*, 9.
[85] R. G. Larson, *Journal of Rheology* **2005**, *49*, 1.
[86] C. Clasen, J. P. Plog, W. M. Kulicke, M. Owens, C. Macosko, L. E. Scriven, M. Verani, G. H. McKinley, *Journal of Rheology* **2006**, *50*, 849.
[87] C. Stoltz, J. J. de Pablo, M. D. Graham, *Journal of Rheology* **2006**, *50*, 137.
[88] R. De Dier, W. Mathues, C. Clasen, *Macromolecular Materials and Engineering* **2013**, *298*, 944.
[89] Q. Huang, L. Hengeller, N. J. Alvarez, O. Hassager, *Macromolecules* **2015**, *48*, 4158.
[90] M. D. Torres, B. Hallmark, D. I. Wilson, *Food Hydrocolloids* **2014**, *40*, 85.
[91] V. Gauri, K. W. Koelling, *Rheologica Acta* **1997**, *36*, 555.
[92] M. W. Yao, G. H. McKinley, B. Debbaut, *Journal of Non-Newtonian Fluid Mechanics* **1998**, *79*, 469.
[93] G. H. McKinley, T. Sridhar, *Annual Review of Fluid Mechanics* **2002**, *34*, 375.
[94] G. Ascanio, P. J. Carreau, E. Brito-De la Fuente, P. A. Tanguy, *Canadian Journal of Chemical Engineering* **2002**, *80*, 1189.
[95] D. F. James, K. Walters, in *Techniques in Rheological Measurement* (Ed: A.A. Collyer), Springer Netherlands, **1993**, p. 33.
[96] G. H. McKinley, T. Sridhar, *Annual Review of Fluid Mechanics* **2002**, *34*, 375.
[97] G. G. Fuller, C. A. Cathey, B. Hubbard, B. E. Zebrowski, *Journal of Rheology* **1987**, *31*, 235.
[98] S. H. Agarwal, R. S. Porter, *Journal of Applied Polymer Science* **1980**, *25*, 173.
[99] V. M. Gol'dberg, G. E. Zaikov, *Polymer Degradation and Stability* **1987**, *19*, 221.
[100] O. Altintas, M. Abbasi, K. Riazi, A. S. Goldmann, N. Dingenouts, M. Wilhelm, C. Barner-Kowollik, *Polymer Chemistry* **2014**, *5*, 5009.
[101] K. Zhang, H. J. Choi, C. H. Jang, *Colloid and Polymer Science* **2011**, *289*, 1821.
[102] J. A. Odell, A. J. Muller, K. A. Narh, A. Keller, *Macromolecules* **1990**, *23*, 3092.
[103] P. J. Sheth, J. F. Johnson, R. S. Porter, *Polymer* **1977**, *18*, 741.
[104] I. I. Kudish, R. G. Airapetyan, M. J. Covitch, in *Tribology and Interface Engineering Series*, Vol. 48 (Eds: D. Dowson, M. Priest, G. Dalmaz, and A.A. Lubrecht), Elsevier, **2005**, p. 441.
[105] R. L. A. David, M. H. Wei, J. A. Kornfield, *Polymer* **2009**, *50*, 6323.
[106] P. Goodman, *Journal of Polymer Science* **1957**, *25*, 325.
[107] R. S. Porter, J. F. Johnson, *Journal of Applied Physics* **1964**, *35*, 3149.
[108] A. A. Al-Hashmi, R. Al-Maamari, I. Al-Shabibi, A. Mansoor, H. Al-Sharji, A. Zaitoun, *Journal of Applied Polymer Science* **2014**, *131*.
[109] A. Dupas, I. Henaut, J. F. Argillier, T. Aubry, *Oil & Gas Science and Technology-Revue D Ifp Energies Nouvelles* **2012**, *67*, 931.
[110] L. Xue, U. S. Agarwal, P. J. Lemstra, *Macromolecules* **2005**, *38*, 8825.
[111] M. Duan, S. W. Fang, L. H. Zhang, F. X. Wang, P. Zhang, J. A. Zhang, *E-Polymers* **2011**, *11*, 86.
[112] T. Q. Nguyen, H. H. Kausch, *Advances in Polymer Science* **1992**, *100*, 73.
[113] S. A. Vanapalli, S. L. Ceccio, M. J. Solomon, *Proceedings of the National Academy of Sciences of the United States of America* **2006**, *103*, 16660.

[114] U. S. Agarwal, R. A. Mashelkar, *Journal of Non-Newtonian Fluid Mechanics* **1994**, *54*, 1.
[115] A. M. Saitta, P. D. Soper, E. Wasserman, M. L. Klein, *Nature* **1999**, *399*, 46.
[116] Y. Kantor, *Pramana-Journal of Physics* **2005**, *64*, 1011.
[117] D. W. Sumners, S. G. Whittington, *Journal of Physics a-Mathematical and General* **1988**, *21*, 1689.
[118] L. H. Zhang, S. W. Fang, M. Duan, F. X. Wang, P. Zhang, J. A. Zhang, D. Y. Chang, *Journal of Macromolecular Science Part B-Physics* **2011**, *50*, 153.
[119] S. Kheirandish, I. Guybaidullin, W. Wohlleben, N. Willenbacher, *Rheologica Acta* **2008**, *47*, 999.
[120] P. G. Dommersnes, Y. Kantor, M. Kardar, *Physical Review E* **2002**, *66*.
[121] J. J. Cooper-White, R. C. Crooks, K. Chockalingam, D. V. Boger, *Industrial & Engineering Chemistry Research* **2002**, *41*, 6443.
[122] D. A. Z. Wever, F. Picchioni, A. A. Broekhuis, *Progress in Polymer Science* **2011**, *36*, 1558.
[123] S. C. Dou, R. H. Colby, *Journal of Polymer Science Part B-Polymer Physics* **2006**, *44*, 2001.
[124] C. J. Zou, P. W. Zhao, J. Ge, Y. Lei, P. Y. Luo, *Carbohydrate Polymers* **2012**, *87*, 607.
[125] S. Malik, S. N. Shintre, R. A. Mashelkar, *Macromolecules* **1993**, *26*, 55.
[126] S. Hietala, P. Mononen, S. Strandman, P. Jarvi, M. Torkkeli, K. Jankova, S. Hvilsted, H. Tenhu, *Polymer* **2007**, *48*, 4087.
[127] S. A. Ali, Y. Umar, H. A. Al-Muallem, B. F. Abu-Sharkh, *Journal of Applied Polymer Science* **2008**, *109*, 1781.
[128] C. Chassenieux, T. Nicolai, L. Benyahia, *Current Opinion in Colloid & Interface Science* **2011**, *16*, 18.
[129] B. S. Kim, P. T. Mather, *Polymer* **2006**, *47*, 6202.
[130] B. Xu, A. Yekta, M. A. Winnik, K. Sadeghy-Dalivand, D. F. James, R. Jenkins, D. Bassett, *Langmuir* **1997**, *13*, 6903.
[131] H. Tan, K. C. Tam, V. Tirtaatmadja, R. D. Jenkins, D. R. Bassett, *Journal of Non-Newtonian Fluid Mechanics* **2000**, *92*, 167.
[132] P. Kujawa, A. Audibert-Hayet, J. Selb, F. Candau, *Macromolecules* **2006**, *39*, 384.
[133] S. L. Cram, H. R. Brown, G. M. Spinks, D. Hourdet, C. Creton, *Macromolecules* **2005**, *38*, 2981.
[134] J. C. Kennedy, J. Meadows, P. A. Williams, *Journal of the Chemical Society-Faraday Transactions* **1995**, *91*, 911.
[135] A. Tripathi, K. C. Tam, G. H. McKinley, *Macromolecules* **2006**, *39*, 1981.
[136] J. A. Odell, A. Keller, A. J. Muller, *Advances in Chemistry Series* **1989**, 193.
[137] Y. R. Choi, Y. H. Bae, S. W. Kim, *Macromolecules* **1998**, *31*, 8766.
[138] J. Roovers, *Polymer* **1979**, *20*, 843.
[139] T. K. Goh, K. D. Coventry, A. Blencowe, G. G. Qiao, *Polymer* **2008**, *49*, 5095.
[140] S. H. Agarwal, R. F. Jenkins, R. S. Porter, *Journal of Applied Polymer Science* **1982**, *27*, 113.
[141] Y. M. Lee, Y. L. Joo, *Journal of Non-Newtonian Fluid Mechanics* **2006**, *140*, 71.
[142] J. G. H. Cifre, R. Pamies, M. C. L. Martinez, J. G. de la Torre, *Polymer* **2005**, *46*, 6756.
[143] D. A. Z. Wever, F. Picchioni, A. A. Broekhuis, *European Polymer Journal* **2013**, *49*, 3289.
[144] L. J. Fetters, A. D. Kiss, D. S. Pearson, G. F. Quack, F. J. Vitus, *Macromolecules* **1993**, *26*, 647.
[145] W. Sun, F. P. Yu, J. P. He, C. Zhang, Y. L. Yang, *Journal of Polymer Science Part a-Polymer Chemistry* **2008**, *46*, 5518.

[146] S. Merino, L. Brauge, A. M. Caminade, J. P. Majoral, D. Taton, Y. Gnanou, *Chemistry-a European Journal* **2001**, *7*, 3095.
[147] G. M. Pavlov, N. Errington, S. E. Harding, E. V. Korneeva, R. Roy, *Polymer* **2001**, *42*, 3671.
[148] Y. J. Sheng, K. L. Cheng, C. C. Ho, *Journal of Chemical Physics* **2004**, *121*, 1962.
[149] H. F. Zhang, J. P. He, C. Zhang, Z. H. Ju, J. Li, Y. L. Yang, *Macromolecules* **2012**, *45*, 828.
[150] O. K. Kim, R. C. Little, R. L. Patterson, R. Y. Ting, *Nature* **1974**, *250*, 408.
[151] H. J. Zhu, J. H. Luo, O. Klaus, Y. Z. Fan, *Colloids and Surfaces a-Physicochemical and Engineering Aspects* **2012**, *414*, 498.
[152] S. Maiti, K. N. Jayachandran, P. R. Chatterji, *Polymer* **2001**, *42*, 7801.
[153] L. Ye, L. J. Mao, R. H. Huang, *Journal of Applied Polymer Science* **2001**, *82*, 3552.
[154] Y. T. Xu, P. Gao, M. Z. Yang, G. S. Huang, B. J. Wang, *Journal of Macromolecular Science Part B-Physics* **2011**, *50*, 1691.
[155] C. E. Sing, A. Alexander-Katz, *Macromolecules* **2010**, *43*, 3532.
[156] R. Hass, W.-M. Kulicke, in *The Influence of Polymer Additives on Velocity and Temperature Fields* (Ed: B. Gampert), Springer-Verlag, Berlin, **1985**, p. 119.

Figure 1. Chemical structure of a) polyacrylamide, b) hydrolysed polyacrylamide, c) polyethylene oxide and d) general structure of a polyvinyl polymer.

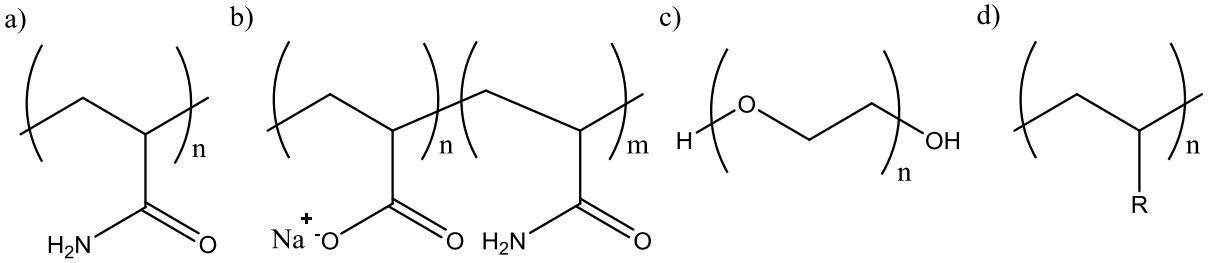

Figure 2. Schematic of single nozzle attached to a boom for agricultural spraying.

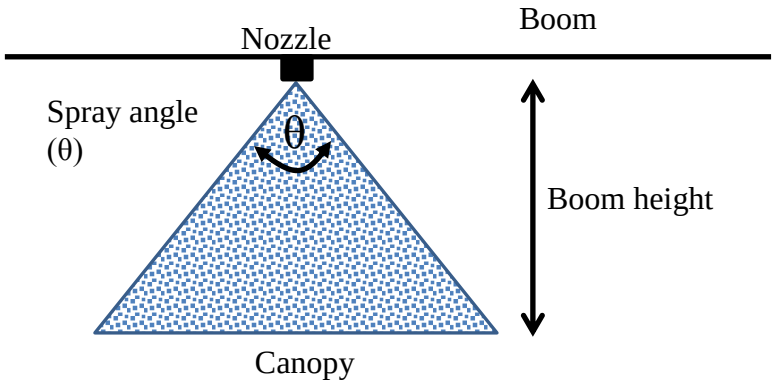

Figure 3. Photographs of fluid jets at ~350 cm s^{-1} of a) a Newtonian fluid, b) a viscoelastic fluid.

Reproduced with permission.[7] Copyright 1998, Elsevier.

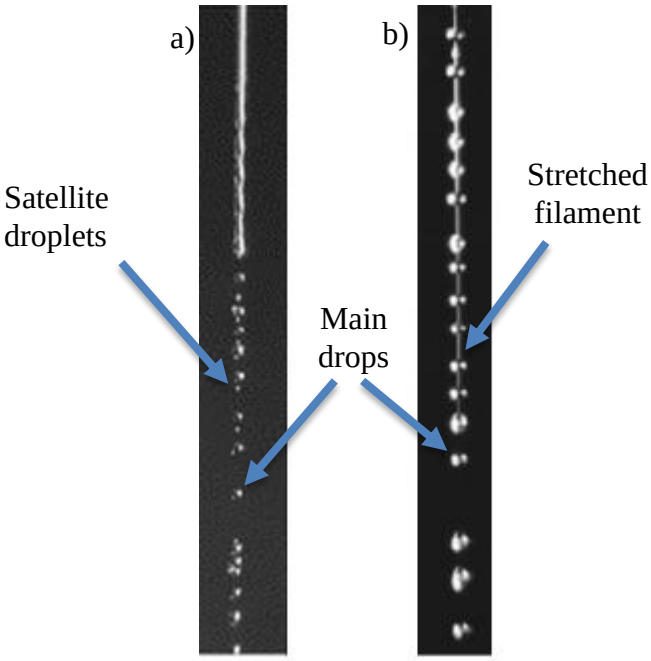

Figure 4. Cylindrical jet breakup at different issuing velocities.

Reproduced with permission. [48] Copyright 2008, Springer.

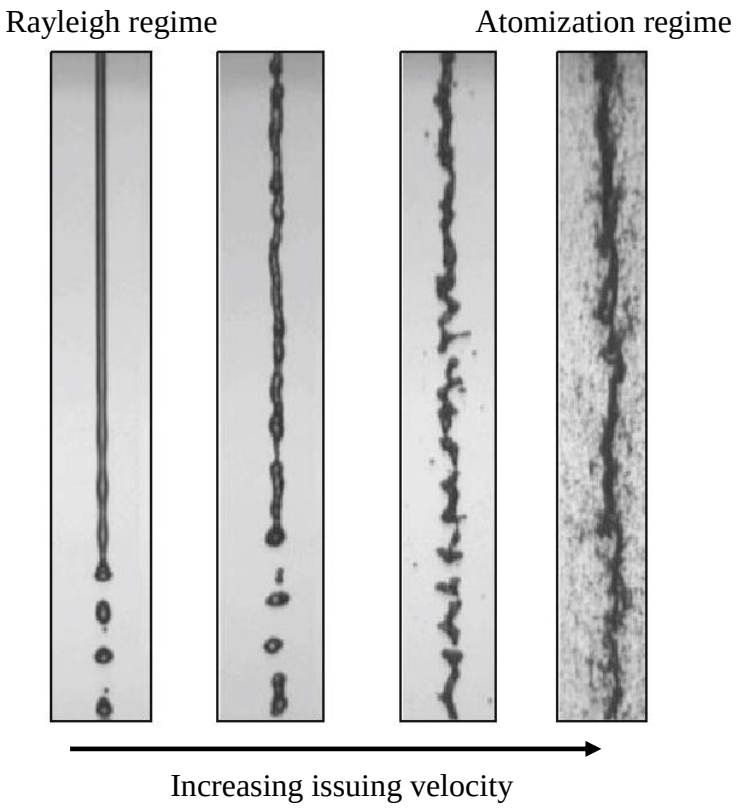

*Figure 5***.** a) Schematic illustration of wave oscillation breakup. b) Photograph of a flat fan nozzle spraying water at 1 bar undergoing oscillation breakup.

a) Reproduced with permission.[50] Copyright 2003, Elsevier.

b) Reproduced with permission.[49] Copyright 1999, Elsevier.

a)

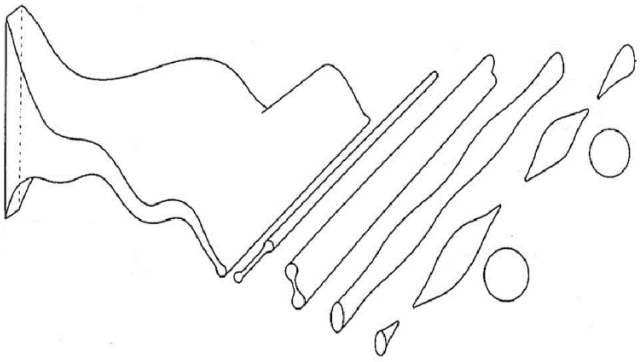

b

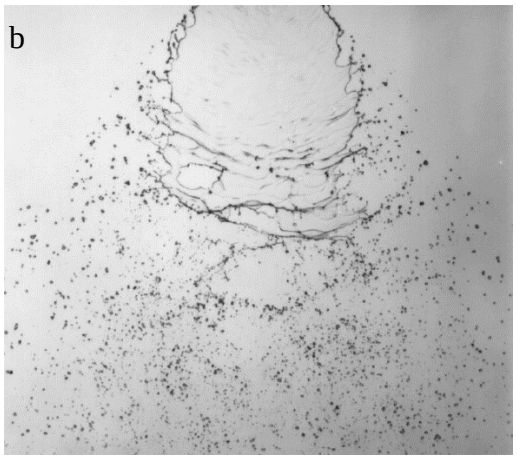

Figure 6. Photograph of a flat fan nozzle undergoing sheet breakup for a) water and b) a viscoelastic wormlike micelle solution.

Reproduced with permission.[55] Copyright 2007, Elsevier.

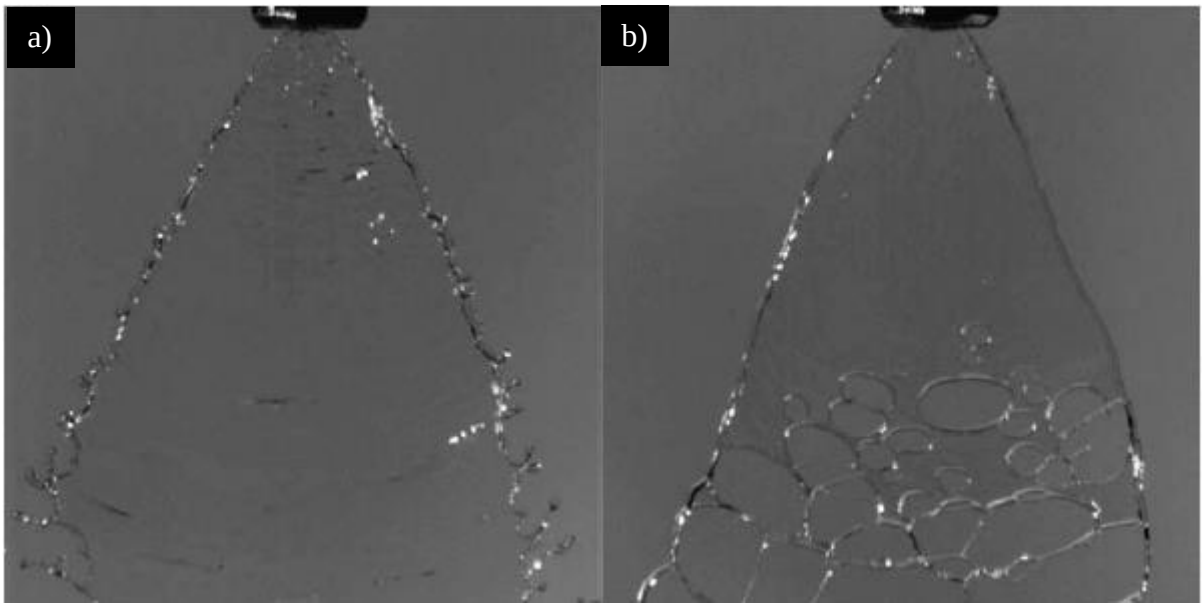

Figure 7. Sketches of viscoelastic filament formations observed during extension.

Reproduced with permission.[59] Copyright 2010, Nature Publishing Group.

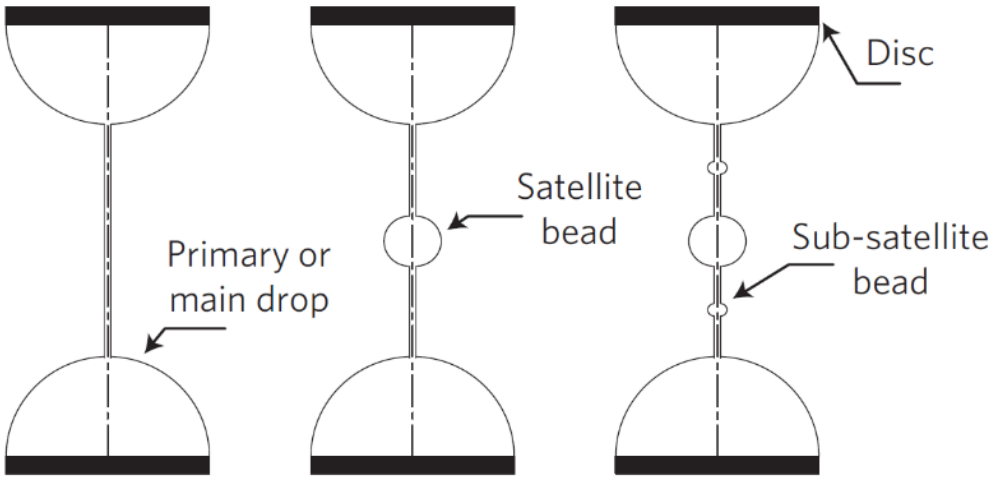

Figure 8. Polymer conformational changes during coil-stretch transition.

Reproduced with permission.[155] Copyright 2010, American Chemical Society.

*Figure 9***.** a) Effect of Weissenberg number on the Tr^+ versus strain plot for dilute polystyrene solutions. b) Polymer contribution to steady-state Tr (divided by concentration and molecular weight) for various polystyrene solutions with increasing Wi.

Reproduced with permission.[75] Copyright 2000, AIP Publishing LLC.

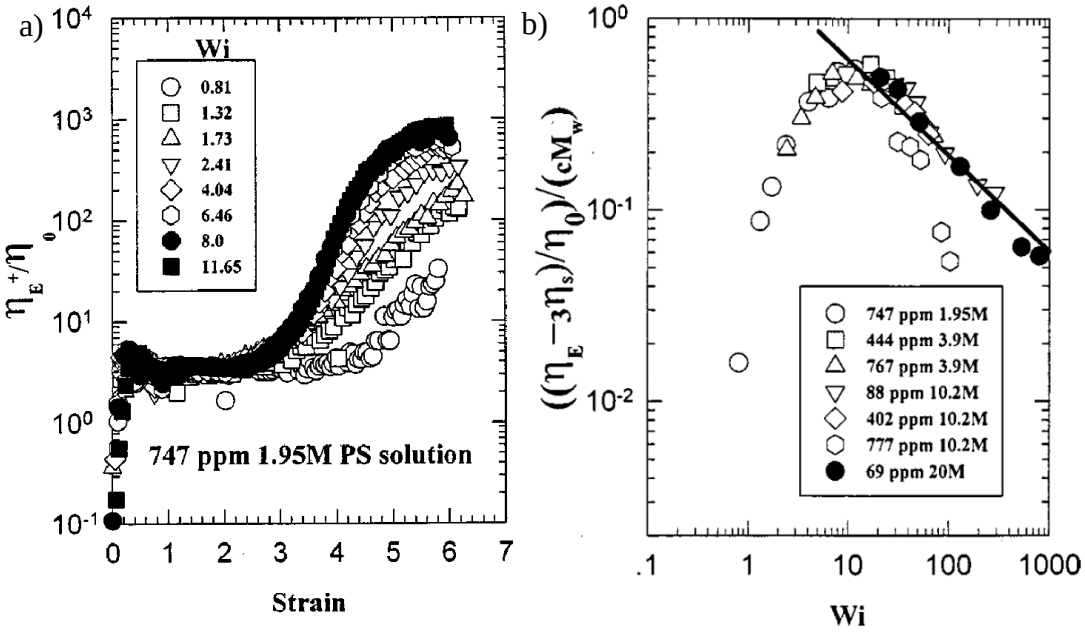

Figure 10. Plot of reduced relaxation time (experimentally measured value divided by the Zimm relaxation time for dilute polymers) of polystyrene solutions at increasing relative concentration.

Reproduced with permission.[86] Copyright 2006, AIP Publishing LLC.

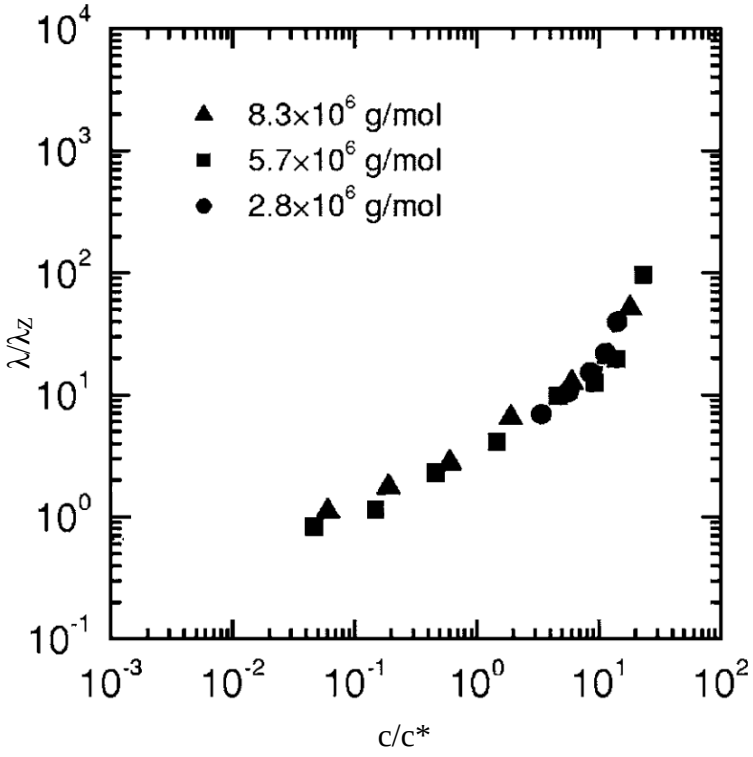

Figure 11. Effect of increasing concentration on normalised steady-state extensional viscosity of high molecular weight polystyrene (PS) solutions at various Wi (where Z is the number of entanglements per chain).

Figure is adapted from data found in figure 5 in reference.[89] Copyright 2006, AIP Publishing LLC.

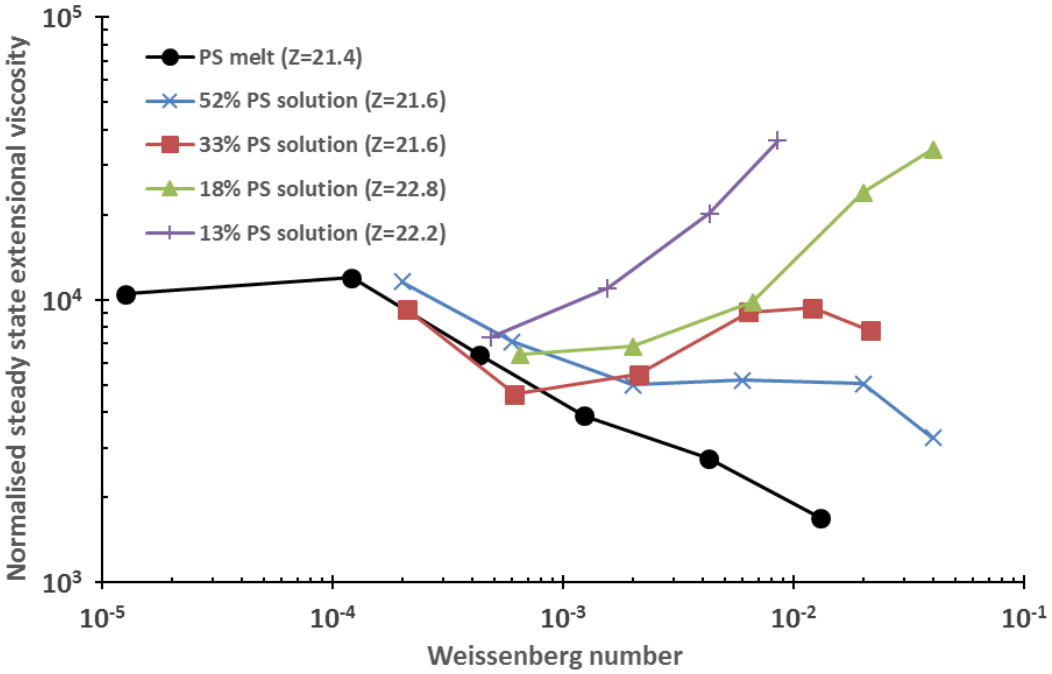

Figure 12. Visual representation of the two main filament stretching failure modes for non-Newtonian fluids: a) necking instability, b) end plate instability.

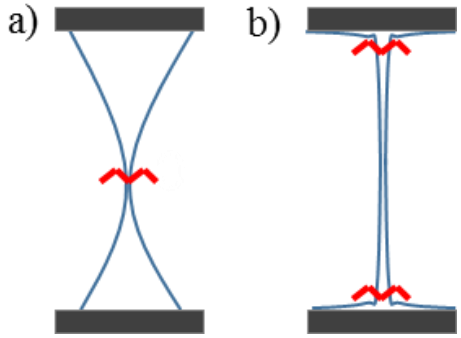

Figure 13. Extensional viscosity measurements of the M1 fluid from various extensional rheometers.

Reproduced with permission.[95] Copyright 1993, Springer.

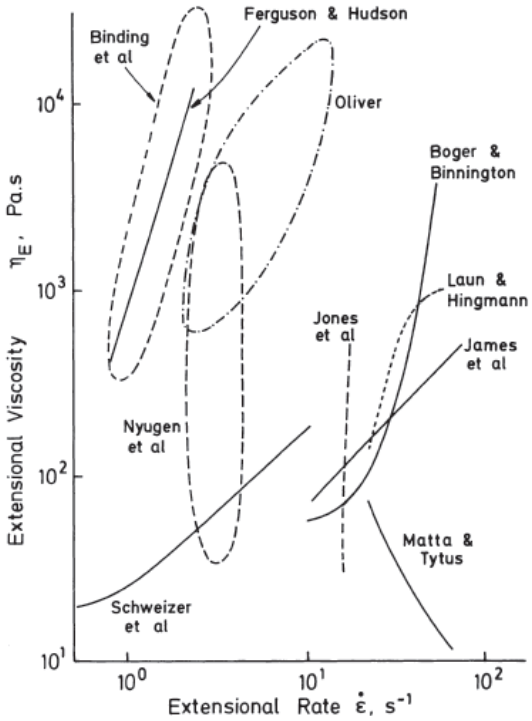

Measuring technique and authors

Fiber spinning
(Binding et al., Ferguson & Hudson, Oliver, Nyugen at al.)

Falling blob
(Matta and Tytus, Jones et al.)

Stagnation point
(Luan & Hingmann, Schweizer et al.)

Converging channel flow
(James et al.)

Contraction flow
(Boger & Binnington)

Figure 14. Polymer degradation associated with the strain hardening process for high molecular weight polystyrene (300 ppm) in toluene during porous media flow.

Figure is adapted from data found in figure 5 in reference[156].

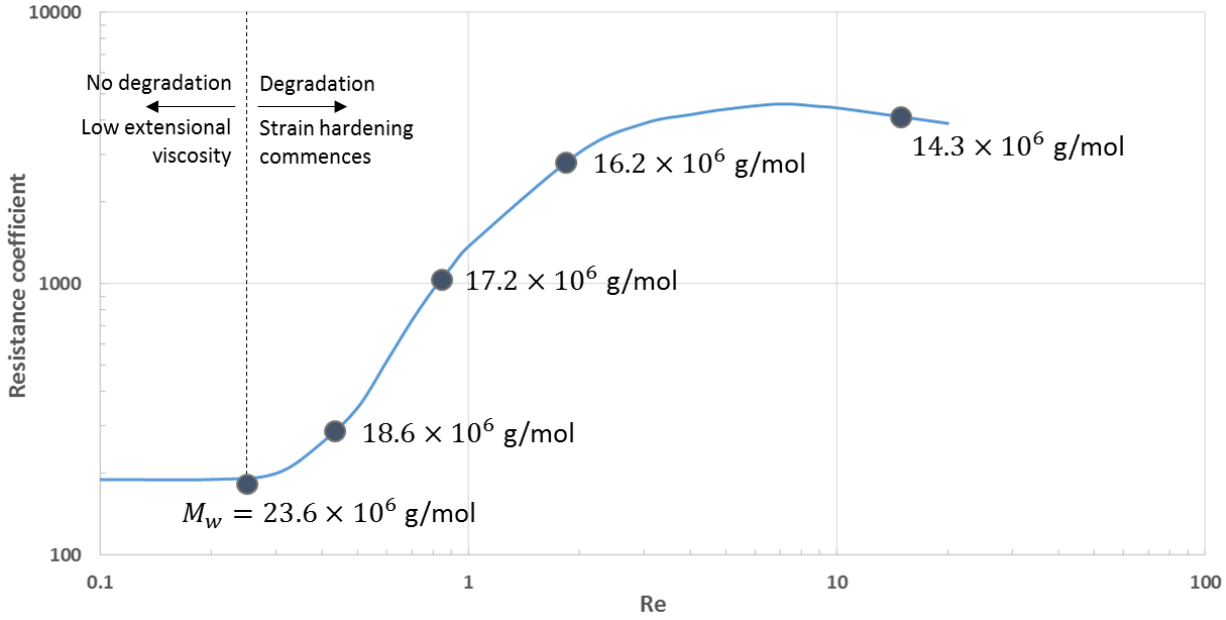

Figure 15. Model stress distribution of a polymer in elongational flow with 2N segments. Reproduced with permission.[110] Copyright 2005, American Chemical Society.

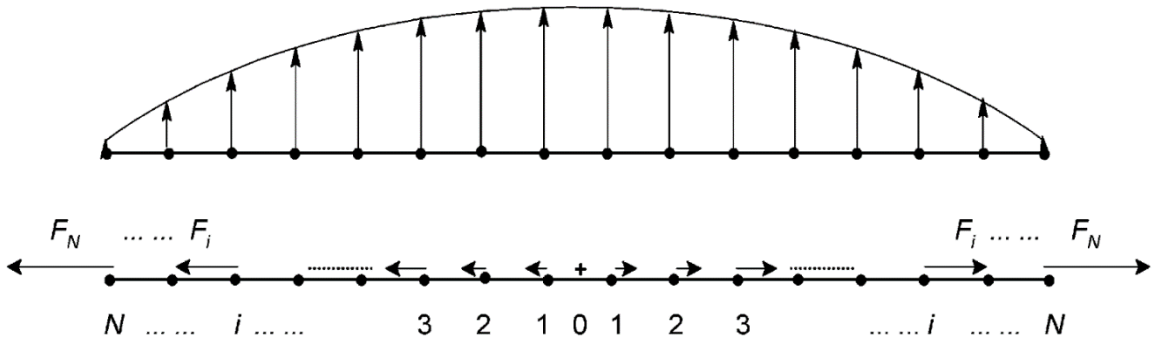

Figure 16. Schematic representation of extended polyelectrolyte confirmation with electrostatic blobs.

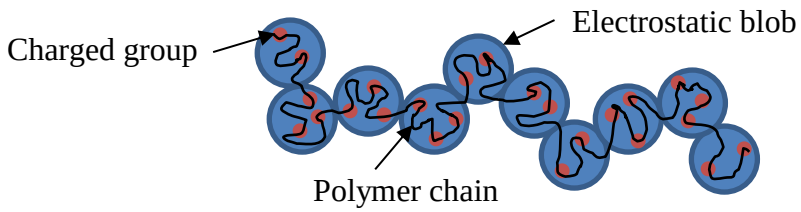

Figure 17. Hydrophobic associative polymers with hydrophobic groups in a) a telechelic arrangement, b) a multi-sticker arrangement.

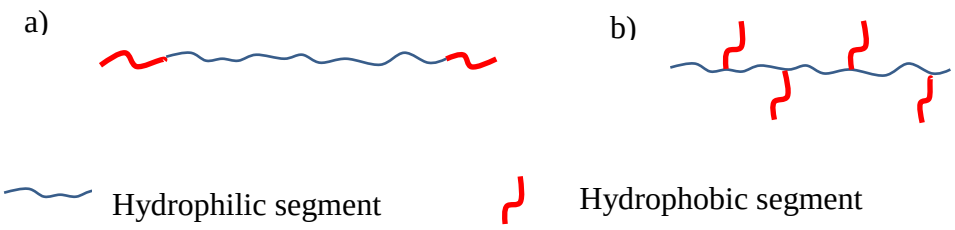

Figure 18. Structure of complementary pairing polymers. a) Acid-functionalised polybutadiene, b) amine-functionalised polybutadiene.

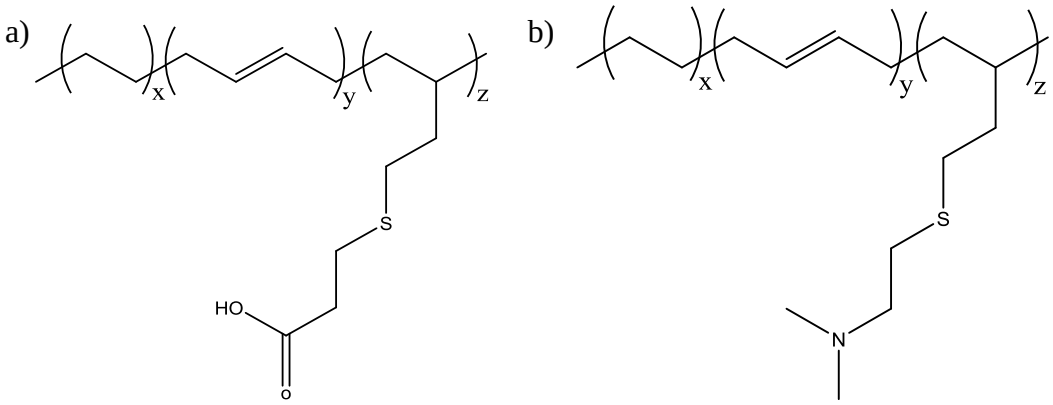

Figure 19. pH sensitive conformation of an ionisable hydrophobically associating polymer. Reproduced with permission.[152] Copyright 2001, Elsevier.

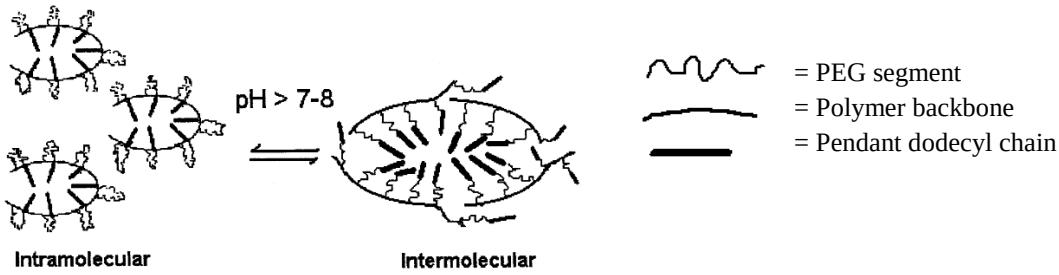

Table 1. Summary of principal functional agents in currently available drift control adjuvants.

Principal Functioning Agent(s)	**Product name (Manufacturer)**
Polyacrylamide	**38-F** (Sanitek Products), **Breeze Ease** (Share Corperation), **Bulls-Eye** (Conklin), **Chem-Trol** (Chemorse), **Control** (GarrCo Products), **Corral Poly** (WinField), **Direct** (Precision Laboratories), **Guide-It** (J.R.Simplot Company), **PointBlank** (Helena Chemical Company), **Reign** (Loveland Products), **Spray-Start** (KALO), **Surewet** (CHemorse), **Syndetic** (Chemorse), **Verimax AMS Dry** (Innvictis Crop Care)
Polyacrylamide (hydrolysed)	**Drift-Gard** (Rosen's Diversified), **Polytex A 1001** (Exacto), **Willowood Driftguard** (Willowood USA)
Polyacrylamide (various)	*Polyacrylamide/ Polysaccharide blend:* **41-A** (Sanitek Products), **Dri-Gard** (Van Diest Supply Company); *Polyacrylamide/ Emulsion blend:* **Affect GC** (United Suppliers); *Polyacrylamide copolymer:* **Gardian** (Van Diest Supply Company), **Poly Dry** (Brewer international)
Polyamides	**Nalco-Trol II** (Nalco Company)
Polyvinyl polymer (unspecified)	**Brandt OnSite** (Brandt), **Clasp** (Helena Chemical Company), **Mist-Control** (Miller Chemical and Fertilizer), **Nalco-Trol** (Nalco Company), **Sta-Put** (Nalco Company)
Poly(ethylene oxide)	**POLYOX** (The Dow Chemical Company)
Unspecified Polymer	**Elite Secure Ultra** (Red River Specialities), **Vector** (Rosen's Diversified)
Polysaccharide	**Array** (Rosen's Diversified), **Border AQ** (Precision Laboratories), **Strike Zone DF** (Helena Chemical Company)
Emulsion (Lecithin based)	**Air Link** (Universal Crop Protection Alliance), **LI 700** (Loveland Products), **Liberate** (Loveland Products), **Prolec** (Brandt)
Emulsion (Vegetable/ Seed oil based)	**Coverage G-20** (Wilbur-Ellis), **Crosshair** (Wilbur-Ellis), **Driftex** (SST Australia), **In-Place** (Wilbur-Ellis), **InterLock** (WinField), **Polytex L 550** (Exacto), **Velomax** (Innvictus Crop Care)
Encapsulation	**Placement** (WinField)

Table 2. Comparison of extensional rheometers used in M1 project in terms of experimental limitations.

Instrument type	**Has shear component**	**Strain rate is not constant**	**Steady state is not reached**	**Has issues with pre-history**	**Limited strain rate/ viscosity**
Fiber spinning	x	x		x	Both
Falling bob		x	x		Both
Stagnation point	x	x	x	x	
Converging channel	x		x		High strain rate
Contraction flow	x	x	x		

Author Biographies

Neil Cameron obtained a BSc and PhD from the University of Strathclyde. Following post-doctoral appointments at TU Eindhoven then Heriot Watt University, he was appointed Lecturer at Durham University in 1997. In 2005 he was promoted to Reader and then in 2008 to Professor in the same department. In September 2014 he became the Monash Warwick Professor of Polymer Materials at Monash University (Australia) and the University of Warwick (UK). His research is focused on the preparation of novel polymeric materials, with particular emphasis on scaffolds for tissue engineering, self-assembling polypeptides, peptide-synthetic polymer hybrids and sugar-containing polymers (glycopolymers).

Reece Lewis completed his Bachelor degree in Chemical Engineering (Honours) at Monash University in 2014. His honours research project was completed with the Ladwig group investigating mixed matrix membranes for gas separation. He then commenced his PhD degree in the Department of Materials Science and Engineering at Monash University. His research interests are focused on the development of novel polymeric materials for industrial application.

Graphical Abstract

Polymeric drift control adjuvants (DCAs) increase the droplet size produced during agricultural spraying which minimizes drift of agrichemicals. Current DCAs are reviewed, highlighting key weaknesses and the mechanism through which they increase droplet size. A discussion on the applicability of new polymer chemistries and architectures to drift control then follows.

R.W. Lewis, R.A. Evans*, N. Malic, K. Saito*, N.R. Cameron*

Polymeric Drift Retardants for Agricultural Spraying